



**INSTITUTO SUPERIOR TÉCNICO**  
Universidade Técnica de Lisboa

# **Model development of a membrane gas permeation unit for the separation of Hydrogen and Carbon Dioxide**

**Diana Fernandes Rodrigues**

## **Dissertação para obtenção do Grau de Mestre em Engenharia Química**

### **Júri**

Presidente: Prof. João Carlos Salvador Santos Fernandes

Orientador: Prof. Maria Norberta Neves Correia de Pinho

Orientador: Prof. Anton Friedl

Vogal: Prof. Maria do Rosário Gomes Ribeiro

**Outubro de 2009**



## Acknowledgments

I would like to thank my supervisors at TU Wien, **Professor Anton Friedl** and **Dr. Walter Wukowits** for their availability, support and patience. I would also like to thank my supervisor at IST **Professor Maria Norberta de Pinho** for her support, kindness and inspiration.

Also at TU Wien I would like to thank everyone at **TVT** research group with special regards to **Aleksander Makaruk** who kindly made the experimental data used in this work available.

During my six months stay in Vienna I had memorable life and work experiences from which I learned a lot and made me grow up as a person. I am very grateful for that but I owe it to all the people I met during this time period. From my office co-workers, **Bettina Liebmman**, **Domenico Foglia** and **Ala Modarresi**, to my friends **Maria de la Vega Muñoz**, **Iván Linares Tomás**, **Julio Jiménez**, **Alex Watson** and **Monica Ralph** and flatmates **Mahmud Reyad** and **Chingfang Wu** (in no particular order), everyone contributed indirectly to this thesis whether it was with a warm smile on a cold day or dinner or good company.

Apart from the six months I was abroad there are a number of people in Lisbon, Portugal and at IST that inspire me and, in a way, they were always with me during my stay in Austria. For that I would like to mention **Sérgio Daniel da Cruz Serra** who I am very thankful for his love and support, **Rita Paixão** for her ever-growing and uplifting good mood, **Joana Teixeira Coutinho** for her kindness and friendship, **Carlos Rodrigues** for his dark humor and company, **Joana Batista** for her timeless friendship, **Ana Tomás** for some nice tunes, **João da Terra** for his nice words, **Maria Teresa Oliveira** for her cleaning skills, **Angela Serrano** for her visit, **Ana Sofia Guedes** for good time, **Ana Filipa Dionísio** for her patience as well as support and **Duarte Neiva** for his good humor and personality. I would also like to mention my final project colleagues **Ana Monteiro**, **Daniel Jacinto** and **Catarina Santos**,

Last but not the least I would like to thank my parents **Gualdino Rodrigues** and **Regina Fernandes** as well as my dog **Puffy** for being my family.

## Resumo

**Palavras-chave:** Membranas, permeação gasosa, Aspen Plus, Aspen Custom Modeller, bio-hidrogénio, separação de hidrogénio e dióxido de carbono .

Neste trabalho foram desenvolvidos três modelos diferentes para uma unidade de permeação gasosa de membranas recorrendo ao software Aspen Custom Modeler. Estes modelos basearam-se no mecanismo de transporte de solução-difusão e descrevem um módulo simples. Dois dos três modelos construídos discretizam o módulo enquanto que o restante considera o módulo como um bloco. Os resultados destes modelos para a separação de uma mistura de metano e dióxido de carbono foram comparados com dados experimentais para validação e concluiu-se que os módulos que têm em conta a discretização produzem os melhores resultados. Um dos modelos discretizado foi usado para efectuar uma análise de sensibilidade à separação da mistura de hidrogénio e dióxido de carbono com uma membrana de PDMS. Foi também elaborada uma breve exposição da tecnologia de membranas disponível para a separação de hidrogénio e dióxido de carbono.

## Abstract

**Keywords:** Membranes, gas permeation, Aspen Plus, Aspen Custom modeller, bio-hydrogen, hydrogen and carbon dioxide separation.

In this work were developed three different membrane gas permeation unit models in Aspen Custom Modeller. These models were based in the solution-diffusion mechanism and describe a single membrane module. Two of the three models built, considered a discretization of the membrane's module whereas the other model considered the membrane as a block. The models' results were compared against experimental data measured from the separation of carbon dioxide and methane for validation. The model that presented itself to be the most suitable one was used on sensitivity analysis calculations for the separation of hydrogen and carbon dioxide with a reverse-selective PDMS membrane. In addition to this, a short overview on membrane technology available for the separation of hydrogen and carbon dioxide was made. The models that provided the best results in validation were the discretized ones.

# Table of Contents

1.	Introduction .....	14
1.1.	Theme and definition .....	14
1.2.	Approach and workflow .....	15
2.	Background.....	16
2.1.	Transport Mechanisms .....	17
2.2.	The Solution-Diffusion Model.....	18
2.3.	Single-Stage and Multi-stage Membrane Processes .....	21
2.4.	Membrane System Designs.....	23
2.4.1.	Plate-and-frame Module .....	23
2.4.2.	Spiral-wound Module .....	24
2.4.3.	Tubular Module .....	24
2.4.4.	Capillary Module .....	25
2.4.5.	Hollow-fiber Module .....	25
3.	Membranes for Gas Separation .....	26
4.	State-of-the-art.....	27
5.	Model Development.....	29
5.1.	Aspen Plus .....	29
5.2.	Aspen Custom Modeller .....	30
5.3.	Comparison between the different modelling tools.....	31
6.	Procedure .....	33
6.1.	Software.....	33
6.2.	Solver settings in ACM and AP.....	34
6.3.	Implementation .....	34
6.3.1.	Model 1 .....	34
6.3.2.	Model 2 .....	36

6.3.3. Model 3 .....	37
6.4. Setting up the components .....	39
6.5. Writing the code .....	39
6.6. Building the icons .....	40
6.7. Setting the variables .....	41
6.8. Exporting the model to Aspen Plus .....	42
6.9. Simulation environment in Aspen Plus .....	43
7. Results .....	44
7.1. Experimental Validation .....	44
7.1.1. Model 1 .....	45
7.1.2. Model 2 .....	47
7.1.3. Model 3 .....	49
7.2. Comparison between the models .....	51
7.3. Sensitivity Analysis - Hydrogen recovery and molar fraction in retentate vs. membrane area .....	53
8. Summary and Conclusions .....	57
9. Literature .....	59
10. Appendix .....	61
10.1. Troubleshooting the export of an ACM model to AP .....	62
10.2. Tips on using ACM .....	63
10.3. Models' Source Codes .....	64
10.3.1. Model 1 .....	64
10.3.2. Model 2 .....	65
10.3.3. Model 3 .....	67

## List of Figures

Figure 1. Hyvolution project scheme .....	14
Figure 2. Membrane set-up .....	16
Figure 3. Flow arrangements in membrane modules.....	21
Figure 4. Single-stage membrane processes.....	22
Figure 5. Two-stage membrane process as simple split up of single stage process .....	22
Figure 6. Two-stage membrane process with permeate recycle .....	22
Figure 7. Two-stage membrane process with cascade.....	23
Figure 8. Schematic drawings of plate-and-frame-modules.....	23
Figure 9. Schematic drawings of a Spiral-wound Module .....	24
Figure 10. Schematic drawings of a tubular module .....	24
Figure 11. Two schemes of capillary modules .....	25
Figure 12. Schematic drawing of a hollow-fiber module.....	25
Figure 13. User Model Library in Aspen Plus.....	29
Figure 14. Simulation window description in ACM .....	31
Figure 15. Schematic drawing of Model 1 .....	35
Figure 16. Input of Model 1 in ACM.....	35
Figure 17. Schematic drawing of Model 2 .....	36
Figure 18. Input of Model 1 in ACM.....	37
Figure 19. Schematic drawing of Model 3 .....	37
Figure 20. Input of Model 3 in ACM.....	38
Figure 21. Variable definition In ACM.....	39
Figure 22. Variable, domain and distribution definition in ACM .....	39
Figure 23. Schematic drawing of Model 1 .....	40
Figure 24. Schematic drawing of Model 2 .....	41
Figure 25. Schematic drawing of Model 3 .....	41



Figure 26. Specification Status window in ACM.....	41
Figure 27. Model 2 in AP simulation environment.....	43
Figure 28. Block options of ACM model exported to AP in AP simulation environment .....	43
Figure 29. Experimental set-up of the membrane used in the validation .....	44
Figure 30. Permeate flow vs. Feed Flow obtained with Model 1 and experimental data.....	45
Figure 31. Retentate flow vs. Feed Flow obtained with Model 1 and experimental data.....	46
Figure 32. Methane concentration vs. Feed Flow obtained with Model 1 and experimental data .....	46
Figure 33. Permeate flow vs. Feed Flow obtained with Model 2 and experimental data.....	47
Figure 34. Retentate flow vs. Feed Flow obtained with Model 2 and experimental data.....	47
Figure 35. Methane concentration vs. Feed Flow obtained with Model 2 and experimental data .....	48
Figure 36. Permeate flow vs. Feed Flow obtained with Model 3 and experimental data.....	49
Figure 37. Retentate flow vs. Feed Flow obtained with Model 3 and experimental data.....	49
Figure 38. Methane concentration vs. Feed Flow obtained with Model 3 and experimental data .....	50
Figure 39. Comparison between models for the results of permeate flow vs. feed flow.....	51
Figure 40. Comparison between models for the results of retentate flow vs. feed flow.....	51
Figure 41. Comparison between models for the results of methane concentration vs. feed flow.....	52
Figure 42. CO <sub>2</sub> recovery vs H <sub>2</sub> loss to permeate for fixed areas increasing the pressure of permeate.....	54
Figure 43. CO <sub>2</sub> recovery vs H <sub>2</sub> loss to permeate for fixed permeate pressures and increasing area.....	55
Figure 44. CO <sub>2</sub> recovery vs H <sub>2</sub> loss to permeate.....	55

**List of Tables**

Table 1. Computer characteristics ..... 33

Table 2. Software Versions ..... 33

Table 3. Port description and base units ..... 40

Table 4. Membrane properties and component permeances ..... 45

Table 5. Membrane parameters ..... 53

Table 6. Feed composition and operating conditions ..... 54

## List of symbols and abbreviations

### Abbreviations

<b>ACM</b>	Aspen Custom Modeller
<b>AP</b>	Aspen Plus
<b>CVD</b>	Chemical Vapour Deposition
<b>PVD</b>	Physical Vapour Deposition
<b>PSA</b>	Pressure Swing Adsorption
<b>EG</b>	Ethylene Glycol
<b>EO</b>	Ethylene Oxide
<b>PEG</b>	Polyethylene Glycol
<b>PEO</b>	Polyethylene Oxide
<b>PMP</b>	Poly-4-methyl-2-pentine
<b>PPG</b>	Polypropylene Glycol
<b>USA</b>	United States of America
<b>VB</b>	Visual Basic
<b>DOF</b>	Degrees of Freedom

## List of symbols and abbreviations (cont.)

### Symbols

$c_i$	Mole concentration of component $i$
$c_{i0}$	Mole feed concentration of component $i$
$c_{i0(m)}$	Mole feed concentration of component $i$ at the membrane's interface
$c_{i\ell(m)}$	Mole permeate concentration of component $i$ at the membrane's interface
$D_i$	Fick's Law Diffusion Coefficient of component $i$
$J_i$	Membrane flux of component $i$
$K_i^G$	Gas phase/membrane phase sorption coefficient of component $i$
$L_i$	Coefficient of component $i$
$\ell$	Membrane thickness
$p$	Pressure
$p_i$	Partial pressure of component $i$
$p_i^o$	Standard partial pressure of component $i$
$p_i^{sat}$	Saturation pressure of component $i$
$p_0$	Feed pressure
$p_{i0}$	Partial feed pressure of component $i$
$p_{i\ell}$	Partial permeate pressure of component $i$
$P_i, P_j$	Permeabilities of components $i$ and $j$
$R$	Ideal gas constant
$T$	Temperature

$Q_i$	Permeance of component $i$
$\mu_i$	Chemical potential of component $i$
$\mu_i^o$	Standard Chemical potential of component $i$
$\gamma_i$	Activity coefficient of component $i$
$v_i$	Molar volume of component $i$
$\alpha_{i/j}$	Selectivity of component $i$ in relation to component $j$
$F_{feed}$	Membrane Feed Flow
$F_{permeate}$	Membrane Permeate Flow
$F_{retentate}$	Membrane Retentate Flow
$y_{i,feed}$	Component $i$ molar fraction in the feed
$y_{i,permeate}$	Component $i$ molar fraction in the permeate
$y_{i,retentate}$	Component $i$ molar fraction in the retentate
$A_{membrane}$	Membrane's area
$P_{feed}$	Feed total pressure
$P_{permeate}$	Permeate total pressure
$k$ (superscript)	Membrane module number
$k$	Constant
$R$ (superscript)	Retentate
$P$ (superscript)	Permeate
$R(x)$	Retentate along membrane's length
$P(x)$	Permeate along membrane's length

$x$	Membrane's length axis
$H$	Height
$A$	Area



A great deal of research at the moment is concerned with the selection of micro-organisms, optimisation of yield and rate of Hydrogen production as well as reactor design. Only a few studies are aiming at the design of feedstock pre-treatment, gas upgrading and additional process steps to successfully combine both fermentation processes and removal of Hydrogen from the fermentation broth.

In order to obtain pure Hydrogen, Carbon Dioxide has to be separated from the product gas. Due to the pressure level of the produced gas, vacuum swing adsorption was initially selected as state-of-the-art gas-upgrading method, being able to cope with fluctuating gas flow rates due to the day/night-cycle in the photo-heterotrophic fermenter. During project work it turned out that for proper operation of the thermophilic fermenter Hydrogen's partial pressure had to be reduced. However, this changed significantly the gas composition up to higher percentage values of Carbon Dioxide. Additionally, the gas-upgrading system had to cope with changing gas-flow rates since the second fermentation step (photo-heterotrophic fermenter) only produces Hydrogen during day but not during night. Under these conditions, adsorption operates with high energy demand and high Hydrogen losses. In addition to amine-scrubbing, which needs a high heat demand for regeneration of the absorption-liquid, membrane processes seem to be a good alternative for upgrading the raw product gas from Hyvolution-process.

To attain not only an economic but also competitive overall process for the non-thermal production of Hydrogen from biomass, a circumspect selection of upstream and downstream processes is necessary. Process simulation is used to select process routes by comparing the performance of different unit operations and design options for the necessary process steps. It will help during integration and optimisation of the selected process route and provide necessary data for process engineering and cost estimation.[1-7]

The final purpose of this work was to build a model for a gas upgrading unit to be used in process simulation in order to perform calculation concerning the separation of hydrogen and carbon dioxide.

## **1.2. Approach and workflow**

In order to build the model of a membrane permeation unit to be used in process simulation it is necessary to know, on a first step, which equations to write, which software to use and how the software works. The second step is validation with experimental data and testing, the final step result calculation.

Firstly, a review of membrane systems available for the separation was made to know the type of membranes used in Hydrogen and Carbon Dioxide separation as well as the equations that govern the transport mechanisms. In addition to this, a brief evaluation of the selected modelling tools was made so to decide which presents to be the most suitable one in order to develop a unit model that is suitable for the Hyvolution project.

Since that there was no experimental data available for the Hydrogen separation, the first model was build for the Methane and Carbon Dioxide system. After validation and testing for this gaseous pair and, assuming that the successful output for this mixture could be extrapolated to the  $H_2/CO_2$  pair, further calculation were made.



## 2. Background

A membrane is a barrier that allows selective mass transport between two phases by permeating some components more than others, hence promoting the separation of components in a mixture. The phases on either side of the membrane can be liquid or gaseous.

Membrane development started with liquid phase separation processes. The first known recorded membrane experiment was in 1748 and consisted in using a piece of pig's bladder as membrane. On one side of the membrane there was a vessel containing “spirits of wine” and on the other side water. As the water permeated through the bladder faster than the wine, the volume of the vessel increased whereas the amount of water (diluted with wine) on the other side of the membrane decreased.

The concept of separating gases with polymeric membranes is more than a hundred years old, but the widespread use of gas membranes has occurred only recently. The first large-scale gas separation membrane process was used in the mid-1940s by the United States government to separate UF<sub>6</sub> isotopes for nuclear fuel enrichment but the first commercially significant gas separation membranes were introduced later in 1979. Nowadays, there is a large range of developed membranes.

Figure 2 shows a schematic set-up for a membrane. The two sides of the membrane are called feed or upstream side and permeate or downstream side. In practice, permeation can take place in both directions. Generally speaking, feed side and permeate side are chosen consistent with the rule that the permeation of the (most) relevant species takes place from feed to permeate side. The feed side flow is initially called the feed flow. The flow resulting after permeation is called retentate or residue flow. On the permeate side the inlet flow is called sweep flow and the exit flow permeate flow. The sweep flow is optional.[9]

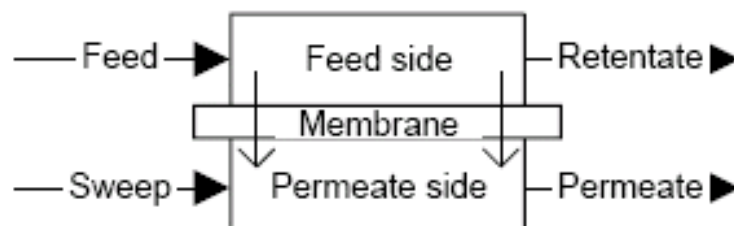


**Figure 2.** Membrane set-up

## 2.1. Transport Mechanisms

The main gas-transport mechanisms through membranes are:

- For porous membranes
  - Poiseuille Flow
  - Knudsen Diffusion
  - Molecular Sieving
  - Capillary Condensation
  - Surface Diffusion
- For dense membranes:
  - Solution-Diffusion

Depending on the properties of the gases as well as the morphology, material and functionality of the various membrane types, one or a combination of these mechanisms fits to explain the gas-transport mechanism of a given separation.

Knudsen diffusion dominates the overall gas-transport in the presence of large Knudsen numbers. The Knudsen number is the ratio of the mean free path of the gas molecules (average distance between collisions) and a representative physical length scale (e.g., the pore radius). The smaller the Knudsen number, the larger the pores become (relative to the mean free path of the gas molecules), the lower selectivity becomes. For Knudsen numbers smaller than one the dominant transport mechanism is viscous flow, which is non-selective.

As far as molecular sieving is concerned, the smaller molecules permeate through the membrane whereas larger molecules do not. Separation based in molecular sieving uses the higher diffusion rate for the smaller molecule almost excluding the diffusion rate of the larger molecule.

In the case of capillary condensation, special interactions between the gases and the membrane pore wall exist, resulting in gas condensation within the constriction.

Surface diffusion occurs when gas molecules are significantly adsorbed on the pore surface. The preferentially adsorbed component may diffuse faster than the remaining gases under a pressure gradient.[9]

Generally, gas transport in dense membranes occurs via the solution-diffusion mechanism which is described in greater detail on the next paragraphs.

## 2.2. The Solution-Diffusion Model

In the solution-diffusion model, permeants dissolve in the membrane material and then diffuse through the membrane along a concentration gradient. The separation occurs due to the difference in rates of diffusion that each permeant has through the membrane's material as well as the solubility of each permeant in the membrane's material. The driving forces of pressure, temperature, concentration and electromotive force are interrelated and the overall driving force producing movement of a permeant is the gradient in its chemical potential.

$$J_i = -L_i \cdot \frac{d\mu_i}{dx} \quad (1)$$

All the common driving forces such as gradients in concentration, pressure, temperature and electromotive force, can be reduced to chemical potential gradients and their effect on flux expressed by the equation above. Considering only concentration and pressure gradients, the chemical potential is written as follows.

$$d\mu_i = RT \cdot d \ln(\gamma_i \cdot c_i) + v_i \cdot dp \quad (2)$$

In incompressible phases such as liquid or solid membranes, volume does not change with pressure. Integrating the equation above with respect to concentration and pressure the result is:

$$\mu_i = RT \cdot \ln(\gamma_i \cdot c_i) + v_i \cdot (p - p_{io}) \quad (3)$$

In compressible gases, the molar volume changes with pressure. Using the ideal gas laws integrating the equation above, the result is the following.

$$\mu_i = \mu_i^o + RT \cdot \ln(\gamma_i \cdot c_i) + RT \cdot \ln\left(\frac{p}{p_i^o}\right) \quad (4)$$

To ensure that the reference chemical potential is the same in every equation, the reference pressure is defined as the saturation vapour pressure of a given component  $i$ . The former equations can be rewritten as:

$$\mu_i = RT \cdot \ln(\gamma_i \cdot c_i) + v_i \cdot (p - p_i^{sat}) \quad (5)$$

$$\mu_i = \mu_i^o + RT \cdot \ln(\gamma_i \cdot c_i) + RT \cdot \ln\left(\frac{p}{p_i^{sat}}\right) \quad (6)$$

Several assumptions must be made to define any model of permeation. The first assumption regarding the transport through membranes is that the fluids on both sides of the membrane are in equilibrium with the membrane material at the interface. This means that there is a continuous gradient in chemical potential

from one side to the other side of the membrane. It is implicit that the rates of absorption and desorption at the interface are much higher than the rate of diffusion through the membrane.

This model assumes that the pressure within a membrane is uniform and that the chemical potential across the membrane is expressed only as a concentration gradient.

$$J_i = -L_i \cdot \left( RT \cdot \frac{d \ln(\gamma_i \cdot c_i)}{dx} + \underbrace{\frac{v_i \cdot dp}{dx}}_{\approx 0} \right) \quad (7)$$

The pressure applied across a dense membrane is also considered to be constant at the high pressure value. Consequently, the pressure difference across the membrane is expressed as a concentration gradient within the membrane,

$$J_i = -\frac{RTL_i}{c_i} \cdot \frac{dc_i}{dx} \quad (8)$$

The term before the derivative is called the diffusion coefficient, the equation above can be rearranged to yield Fick's Law.

$$J_i = -D_i \cdot \frac{dc_i}{dx} \quad (9)$$

Integrating (x) along the thickness of the membrane, under steady-state conditions the result is:

$$J_i = \frac{D_i \cdot (c_{i0} - c_{i\ell(m)})}{\ell} \quad (10)$$

In gas permeation, a gas mixture at a pressure  $p_0$  is applied to the feed side of the membrane, while the permeate gas at a lower pressure  $p_\ell$  is removed from the downstream side of the membrane. Considering that the chemical potentials at either side of the gas/membrane interface is the same and therefore stating that equation 5 equals 6:

$$\mu_i^o + RT \cdot \ln(\gamma_{i0} \cdot c_{i0}) + RT \cdot \ln\left(\frac{p_0}{p_i^{sat}}\right) = \mu_i^o + RT \cdot \ln(\gamma_{i0(m)} \cdot c_{i0(m)}) + v_i \cdot (p - p_i^{sat}) \quad (11)$$

These equations can be rearranged to

$$c_{i0(m)} = \frac{\gamma_{i0}}{\gamma_{i0(m)}} \cdot \frac{p_0}{p_i^{sat}} \cdot c_{i0} \cdot \underbrace{\exp\left(\frac{-v_i(p_0 - p_i^{sat})}{RT}\right)}_{\approx 1} \quad (12)$$

The exponential term is close to one (Poynting correction). The concentration can be expressed as:

$$c_{i0(m)} = \frac{\gamma_{i0}}{\gamma_{i0(m)}} \cdot \frac{p_{i0}}{p_i^{sat}} \quad (13)$$

The concentration of component  $i$  at the feed interface of the membrane can be written as follows,

$$c_{i0(m)} = K_i^G \cdot p_{i0} \quad (14)$$

In an analogue way, the concentration of a given component can be shown to be the following.

$$c_{i\ell(m)} = K_i^G \cdot p_{i\ell} \quad (15)$$

Combining equations 10 with 14 and 15, the result is:

$$J_i = \frac{D_i \cdot K_i^G \cdot (p_{i0} - p_{i\ell})}{\ell} \quad (16)$$

The product of the diffusion coefficient by the sorption coefficient (solubility) is the permeability coefficient, leading to:

$$J_i = \frac{P_i \cdot (p_{i0} - p_{i\ell})}{\ell} \quad (17)$$

$$J_i = Q_i \cdot (p_{i0} - p_{i\ell}) \quad (18)$$

$$Q_i = \frac{P_i}{\ell} \quad (19)$$

This equation shows that the flow rate across a membrane is proportional to the difference in partial pressure and inversely proportional to the membrane thickness. The ideal selectivity is given by the ratio of permeability coefficients between two components.

$$\alpha_{i/j} = \frac{P_i}{P_j} \quad (20)$$

The permeability coefficient is a characteristic parameter that is often described as an intrinsic parameter easily available from simple permeation experiments with membranes of known thickness using equation 17.[8]

### 2.3. Single-Stage and Multi-stage Membrane Processes

The simplest membrane processes are single-stage membrane processes. A stage is formed by one or more membrane modules assembled into an operating unit that provides a specific function different from any other membrane stages that may be utilized in the same process.

The basic membrane stage set-up is shown in Figure 2. Although the recovery is high for this kind of operation, it is usually not preferred because non-permeating species increase with time on the feed side, leading to so-called concentration polarization. This means that, with time, the feed side concentration of the permeating specie decreases, reducing the driving force and therewith the transport through the membrane. Instead, cross-flow operations are preferred, such as configurations in which the flows run alongside the membrane. In this set-up, deterioration of membrane flux with time is limited. In general, four cases of cross-flow operations are distinguished:

- Co-current
- Counter-current
- Cross-flow with perfect permeate mixing
- Perfect mixing

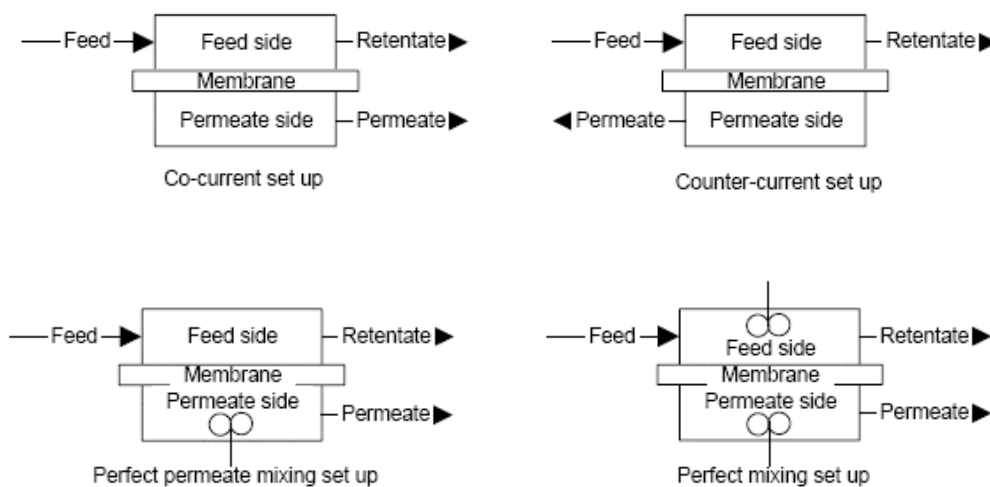


**Figure 3.** Flow arrangements in membrane modules

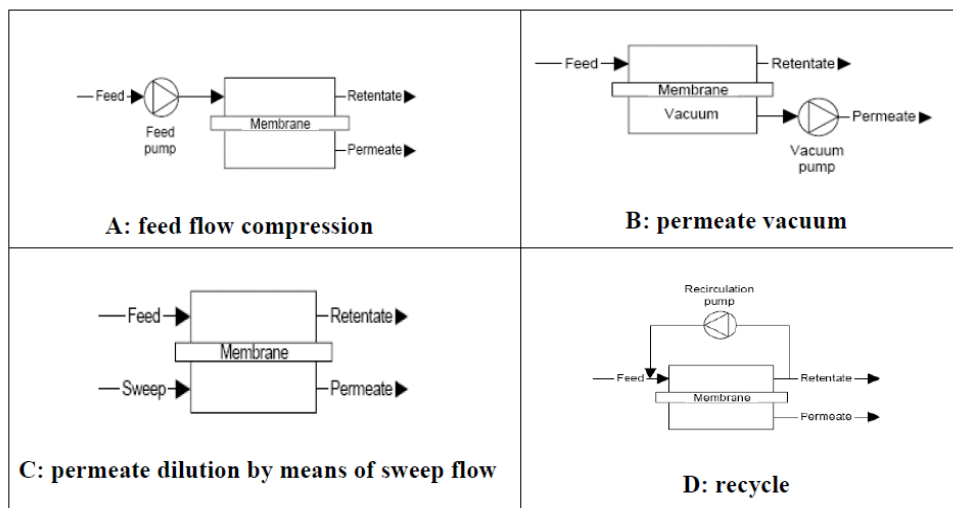


**Figure 4.** Single-stage membrane processes

In order to improve a system's performance, multistage processes can be built. Often, these systems require additional equipment. Nevertheless the improvements in the separation outrun the additional equipment costs.

Most multistage membrane systems incorporate some sort of recycle to enhance product separation and recovery. Such designs are easy to implement from a membrane standpoint, but always require compression for the recycle stream. Gas compression is expensive, but recycling generally improves overall process efficiency

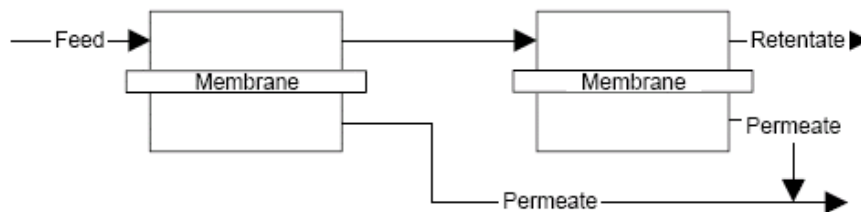


**Figure 5.** Two-stage membrane process as simple split up of single stage process

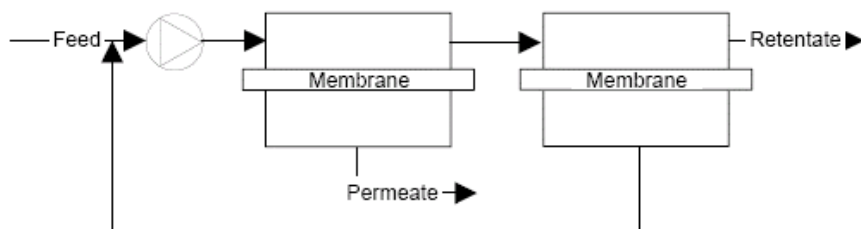


**Figure 6.** Two-stage membrane process with permeate recycle

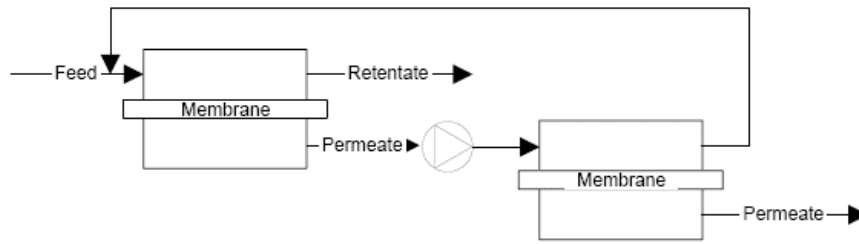


**Figure 7.** Two-stage membrane process with cascade

## 2.4. Membrane System Designs

The building block of a membrane system is called the module. All module types applied so far are based on two types of membrane configurations: flat and tubular. Module types based on flat membranes are the plate-and-frame and spiral-wound modules.

### 2.4.1. Plate-and-frame Module

Plate-and-frame modules are the closest to common laboratory set-ups. They are constructed placing flat membranes parallel to each other. The spacer plate separates the feed flows running alongside different membranes in the module. The stop disc in the right-hand figure is used to improve the flow pattern in order to use the membrane surface as efficiently as possible (to reduce so-called 'channeling', i.e., the tendency of the flow to move along a fixed pathway). The packing density (i.e., membrane surface per module volume) is around  $100\text{--}400\text{ m}^2/\text{m}^3$ .

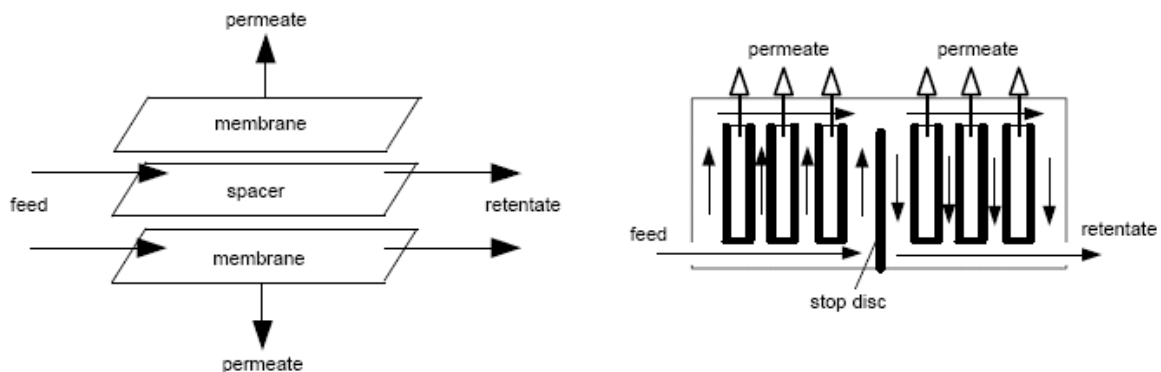


**Figure 8.** Schematic drawings of plate-and-frame-modules



### 2.4.2. Spiral-wound Module

A spiral-wound module is a plate-and-frame system wrapped around a central pipe collecting the permeate. The feed flow runs through the cylinder in axial direction, whereas the permeate runs in radial direction towards the center of the cylinder. The packing density of spiral-wound modules is higher than the packing density of plate-and-frame modules is in the range  $300\text{--}1000\text{ m}^2/\text{m}^3$ , however it depends strongly on the channel height.

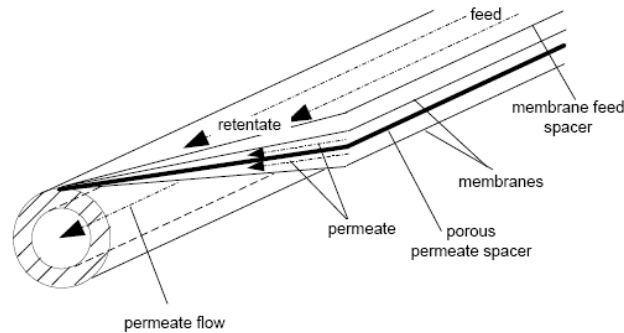


**Figure 9.** Schematic drawings of a Spiral-wound Module

### 2.4.3. Tubular Module

Tubular membranes consist of a thin selective membrane layer deposited on the inside or outside of a tubular support with a diameter generally larger than 10 mm. The number of tubes put together in the module is may vary, The feed flows through the center of the membrane tubes and the permeate crosses the membrane from the inside to the outside, flowing subsequently in the larger tube. The maximum packing density is around  $300\text{ m}^2/\text{m}^3$ .

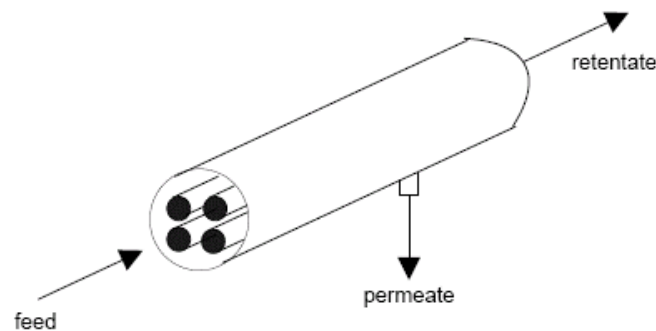


**Figure 10.** Schematic drawings of a tubular module

#### 2.4.4. Capillary Module

The capillaries are self-supporting and bound together at the free ends (potted) with agents such as epoxy resins, polyurethanes, or silicone rubber. The feed flow can go through the bores of the capillaries, with the permeate exiting the membrane sideways (left scheme), but the feed can also run through the capillaries on the outside with the permeate exiting through the bores of the membrane. Packing densities to be attained are in the range  $600\text{-}1200\text{ m}^2/\text{m}^3$ .

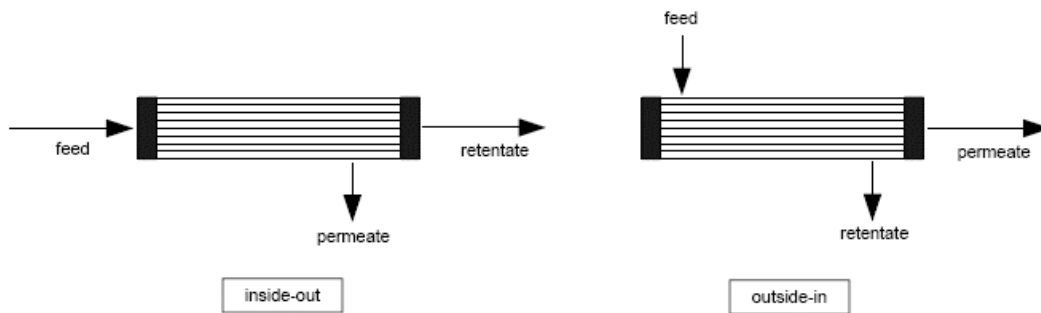


Figure 11. Two schemes of capillary modules

#### 2.4.5. Hollow-fiber Module

The hollow fiber module is essentially the same as the capillary module, only the size of the tubes is smaller. Hollow fibers are self-supporting and resistant to collapse in high pressure and environmentally difficult situations. Amongst all the module types currently available, hollow fiber modules can reach the highest packing density of  $30000\text{ m}^2/\text{m}^3$ . Hollow fiber modules are preferably used when the feed stream is relatively clean. Due to the small bore diameter, pressure losses are relatively high. By selecting the 'outside-in' type pressure losses occurring inside the fibers can be reduced, and a high membrane area can be attained

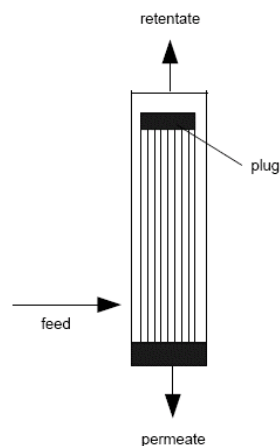


Figure 12. Schematic drawing of a hollow-fiber module

### 3. Membranes for Gas Separation

Whether a membrane is Hydrogen or Carbon Dioxide selective its classification and properties depend on their material and fabrication method. An important result of the recent and rapidly growing interest in gas separation membranes has been the development of a host of new materials specifically designed to enhance gas transmission and permselectivity. While early gas membranes used polymers readily available or borrowed from liquid separation membranes, the current trend is to employ materials with more advanced molecular structures built specifically for gas separations.

Membranes can be classified according to the material they are made of as:

- Polymeric (organic)
- Inorganic (metallic and non-metallic)
- Supported-liquid/facilitated transport
- Mixed-matrix (hybrid)

The choice of a membrane material for gas separation applications is based on specific physical and chemical properties that also depend on the way that the membrane is engineered.

Besides the material, gas separation properties of membranes depend upon:

- The membrane structure and thickness
- The membrane configuration
- The module and system design

The most important membrane manufacturing techniques for gas separation membranes are:

- Sintering
- Track-etching
- Template leaching
- Coating
- Sol-gel process
- Chemical vapor deposition (CVD)
- Physical vapor deposition (PVD)
- Alloy casting and rolling
- Electroless plating and electroplating
- Pyrolysis

Both membrane's permeability and selectivity influence the economics of a gas separation membrane process. Permeability is the rate at which any compound permeates through a membrane; it depends upon thermodynamic factors already exposed in Chapter 2.2. Selectivity is the ratio of permeability coefficients as given in equation 20.

## 4. State-of-the-art

Glassy polymers are generally used for H<sub>2</sub>-selective membranes and show higher thermal stability than rubbery polymers, which are used for CO<sub>2</sub>-selective membranes. Ergo, H<sub>2</sub>-selective membranes can be used with higher operating temperatures when compared with rubbery polymers. In addition to this, H<sub>2</sub>-selective membranes are able to handle higher compression in feed streams and work predominantly on the principle of diffusivity selectivity; the higher diffusivity of H<sub>2</sub> (compared to the other gases) ensures the exclusion of other gases. A serious drawback of H<sub>2</sub>-selective membranes for hydrogen purification is the need to recompress the permeate stream after separation which is highly energy demanding, and therefore may overturn the economic advantages of membrane-based separations compared to PSA or cryogenic distillation. Furthermore, the gas-separation performance of glassy polymeric membranes deteriorates significantly in the presence plasticizing gases. However, the plasticization effects can be reduced to certain degree by various approaches including chemical crosslinking.

A distinct economic advantage of CO<sub>2</sub>-selective membranes is the elimination of the recompression of H<sub>2</sub> since it remains in the high-pressure retentate stream. Moreover, the CO<sub>2</sub>- plasticization at high operating pressures does not compromise the separation performance of CO<sub>2</sub>-selective polymeric membranes. The presence of other plasticizing components, for instance, H<sub>2</sub>S and H<sub>2</sub>O, may not interfere with the purification of H<sub>2</sub>. Indeed, simultaneous improvements in CO<sub>2</sub>/H<sub>2</sub> selectivity and CO<sub>2</sub> permeability may be achieved with plasticization effects. Another feature of CO<sub>2</sub>-selective membranes is that they cannot be employed under high operating temperatures. These membranes generally evidence poorer CO<sub>2</sub>/H<sub>2</sub> selectivity at elevated temperatures. Since the removal of the hydrogen mixture obtained in the Hyvolution process does not need high temperatures, it constitutes an advantage to use CO<sub>2</sub>-selective membranes.

However, a drawback of the reverse selective membranes is that the impurities such as N<sub>2</sub> and O<sub>2</sub> (gases with low condensability) in the feed stream may remain in the retentate stream with H<sub>2</sub>. Additional post-separation processing may be necessary to remove such non-condensable impurities.

Recently, polymers containing ethylene oxide (EO) and/or ethylene glycol (EG) units were found to be suitable for fabricating CO<sub>2</sub>-selective membranes. The enhanced solubility of CO<sub>2</sub> molecules in poly(ethylene oxide) (PEO) accounts for the good CO<sub>2</sub>/light gas selectivity. The CO<sub>2</sub> and H<sub>2</sub> permeabilities of amorphous PEO were estimated to be 140 Barrers and 21 Barrers, respectively at 35°C, and the corresponding CO<sub>2</sub>/H<sub>2</sub> selectivity is 6.8 [19]. One shortcoming of using pure PEO as a membrane material is its strong tendency to crystallize, especially for polymers with high molecular weights. The presence of crystalline structures in polymeric membranes is undesirable for gas separation since these crystals are generally impermeable to gas molecules. To overcome this decrease in permeability due to crystallinity and thus utilize the enhanced CO<sub>2</sub> solubility in PEO, PEO-containing polymers were designed. Okamoto's group [20-22] employed a series of PEO-containing polymers including polyurethanes, polyamides and polyimides for separation applications. Among these polymers, it was found that PEO-containing polyimide membranes showed better gas-separation properties. However, the long-term stability of PEO-containing polyimide is questionable since the

gas-separation performance tends to deteriorate with time. Subsequently, a hyper-branched polyimide containing PEO soft segments was utilized for the separation of CO<sub>2</sub>/H<sub>2</sub>, and a separation factor of 6.2 was obtained.[23]

A potential polymer of interest for fabricating CO<sub>2</sub>-selective membranes is Pebax. It was first introduced as a material for gas-separation membranes by Membrane and Technology Research (MTR) Inc., USA in 1990 [24]. Kim et al. [29] applied Pebax for gas separation and discovered that polarizable gases (e.g. CO<sub>2</sub> and SO<sub>2</sub>) demonstrated higher permeability. The CO<sub>2</sub>/H<sub>2</sub> separation factor is approximately 6.1, and the CO<sub>2</sub> permeability is 130 Barrers at 25 °C. The high CO<sub>2</sub> permeability and CO<sub>2</sub>/H<sub>2</sub> selectivity of the Pebax copolymer are attributed to the flexible polyether segments (PEO) and the rigid amide blocks, respectively. Bondar et al. [25] investigated another series of Pebax polymers for their gas-transport properties, and the highest CO<sub>2</sub>/H<sub>2</sub> selectivity obtained was 10 at 35 °C. Moreover, the CO<sub>2</sub> permeability of the Pebax membranes increased at elevated pressures while H<sub>2</sub> permeability decreased with increasing pressure. Hence, an improvement in the CO<sub>2</sub>/H<sub>2</sub> separation performance of Pebax membranes is achieved at higher pressures.

Simmons [26] synthesized a series of poly(ether-urethane) and poly(ether-urea) block copolymers that contained polypropylene glycol (PPG) or PEG units. The CO<sub>2</sub>/H<sub>2</sub> selectivity of the synthesized materials was comparable to Pebax, but the CO<sub>2</sub> permeability is much larger (590 Barrers). Simmons [27] extended the work by synthesizing novel polyester-polyether block copolymers containing PEG units whereby a CO<sub>2</sub>/H<sub>2</sub> selectivity of 13 and CO<sub>2</sub> permeability of 220 Barrers at 35 °C were achieved. The presence of PEO or PEG units accounts for the preferential transport of CO<sub>2</sub> across these rubbery polymeric membranes. These results suggest that block copolymers containing PEO or PEG are potential materials for CO<sub>2</sub>-selective membranes.

Recent studies have proven that the introduction of polar groups effectively enhances CO<sub>2</sub> solubility, but it may also increase the “size discrimination” ability ( $D_{H_2}/D_{CO_2}$ ) of the membranes. This “size discrimination” property is not desirable for CO<sub>2</sub>-selective membranes as it decreases the acquired gain in solubility selectivity. Currently, ether oxygen among other functional groups gives a good balance between CO<sub>2</sub> permeability and CO<sub>2</sub>/H<sub>2</sub> selectivity. The future discovery of more suitable polar groups that effectively improve selectivity but have neglectable influence on  $D_{H_2}/D_{CO_2}$  is required. Although the majority of the CO<sub>2</sub>-selective polymeric membranes are fabricated using rubbery polymers, there are some glassy polymers that are highly permeable to CO<sub>2</sub>. For instance, Morisato and Pinnau [28] synthesized glassy poly(4-methyl-2-pentyne) (PMP) for gas separation because it has an exceptionally high gas permeability that results from the extraordinarily high free volume and interconnectivity of the free-volume elements. PMP membranes have an extremely large CO<sub>2</sub> permeability of 11,000 Barrers but a poor CO<sub>2</sub>/H<sub>2</sub> selectivity of only 1.8. The large intrinsic CO<sub>2</sub> permeability of PMP membranes allows room for further modification to enhance the gas-pair selectivity. The possible decrease in gas permeability after modification could be more than compensated for by the corresponding increase in gas-pair selectivity, provided that the gas permeability is still reasonable [10-11].

## 5. Model Development

Currently on the market there is a wide range of process simulators for the chemical industry such as Aspen Plus. However, membrane operations are not available in any of these process simulators model libraries. It is therefore necessary to build a custom unit operation.

When building a model to use in a process simulator, a number of questions has to be answered such as:

- Is it necessary to know any programming language?
- Is the modelling environment equation-oriented?
- Is it third-party software?
- How is it exported to other platforms?

The answer to these questions depends to a great extent on the goals and applications of the model itself as well as the people who wish to develop it.

The first thing taken into account was that the model should be suited for the sequential modular simulator Aspen Plus. Knowing this, it was possible to narrow down the modelling environment options that are described in the paragraphs below.

### 5.1. Aspen Plus

In the model library of Aspen Plus it is possible to identify the section User Models. In this section three different user models are present: User Model , User Model 2 and User Model 3.

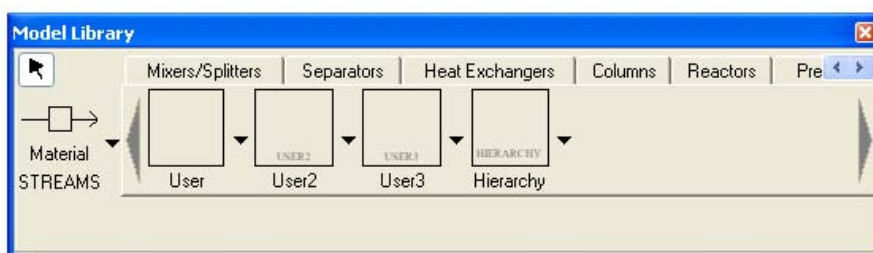


**Figure 13.** User Model Library in Aspen Plus

Each one of these user models can be linked with Microsoft Excel, Fortran or both to build a custom model for the model library of Aspen Plus.

All of them use FORTRAN as programming language, but *User2* offers the possibility of a combination with an Excel file. *User3* models are used to simulate features that are not in the standard Aspen Plus models. *User* and *User2* differ only in the number of inlet and outlet streams allowed and the argument lists to the

model subroutine. User is limited to a maximum of four material and one heat or work inlet stream and a maximum of four material and one heat or work outlet stream. User2 has no limits on the number of inlet and outlet streams.

To build a model using User2 and an Excel file Aspen Plus offers a template delivered with the software package, showing how to exchange the necessary data between Aspen and Excel and vice versa.

Aspen also supplies a template with FORTRAN code to model a hollow fibre membrane unit that can be customized in order to create the desired subroutine. The description of the code and its arguments are shown in great detail in [12-14].

Generally speaking, what happens internally when linking Excel or Fortran files with Aspen is that the model's variables, equations and parameters are defined in the Excel or Fortran file and, in the case of Fortran, the subroutines that are called in the code are the instruments that serve as the linking platform between Aspen and Fortran. In the case of Excel are the contained macros in visual basic that contain the Aspen Helper functions that contain the information for the transfer between Aspen and Excel.

After developing the models in Excel or FORTRAN there is the possibility to insert the models in the Aspen Plus User Model Library permanently with their own icon and designation so that the developed unit operation can be used in various flowsheets. Using Visual Basic, the model can be turned into a form in Aspen Plus, which means that a new unit operation model can figure the Model Library with the respective setup folders for inputs and outputs. The detailed explanation on how to do that can be found in [12-14].

## **5.2. Aspen Custom Modeller**

ACM can be set apart from the other modelling tools because it uses an object-oriented modelling language, editors for icons and tasks, and Microsoft Visual Basic for scripts. ACM is customizable and has extensive automation features, making it simple to combine with other products such as Microsoft Excel and Visual Basic.

Since this was the chosen environment to develop the model of the gas permeation unit its feature will be present in more detail.

In Figure 14 a brief explanation of the options available in the working environment is presented.

The main elements of the interface are:

- The Flowsheet window
- The Simulation Messages window
- The Simulation Explorer

The simulation messages window, as the name suggests, gives the status of the current simulation and the simulation explorer is basically where the tools to build the model can be found. The procedure on how to start building a model is shown in [12-15].

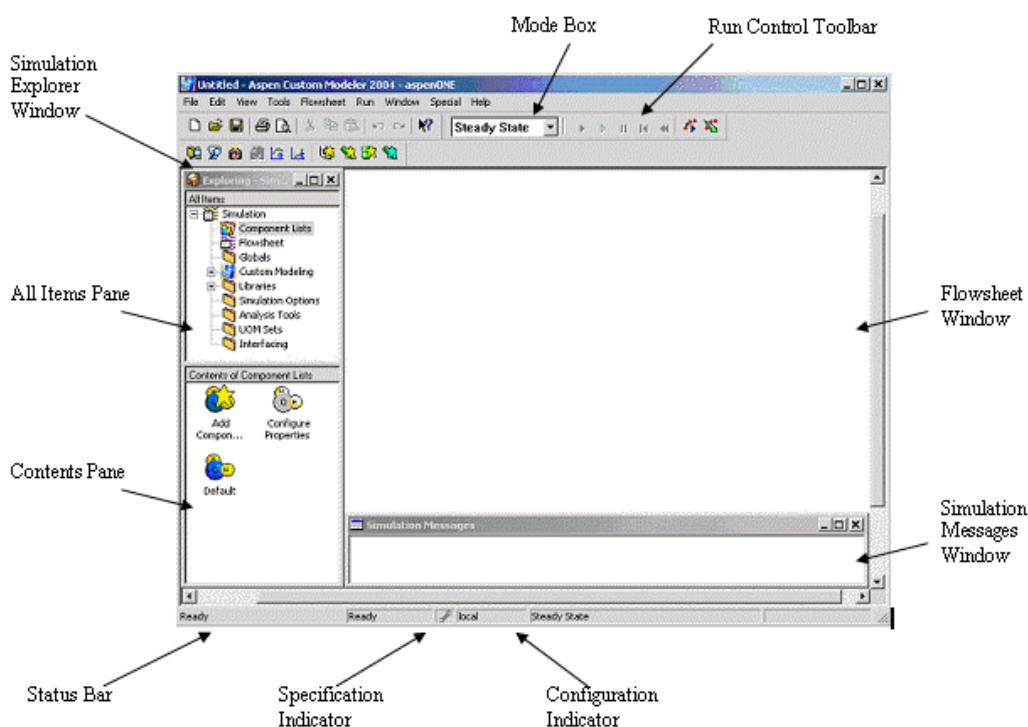


**Figure 14.** Simulation window description in ACM

### 5.3. Comparison between the different modelling tools

It is possible to break down the modelling in Aspen Plus in three different levels being the first level implementing the model equations, variables, integer and real parameters, the second level would be implementing the created model in the Aspen Model Library and the third create an Aspen Custom form which has the versatility to deal with input and results without using third-party software. It is also possible to separate the modelling in Excel, FORTRAN or both from ACM because the first two need the User model in the Aspen Model Library and ACM does not.

As far as implementing the model's equations and parameters is concerned, to build the model in Excel is by far the most user-friendly option not only because of the well-known Excel interface but also because of the template file made available by Aspen Plus. In addition to this, the model built in Excel is easier to test and troubleshoot since it is self-contained and doesn't require in-depth FORTRAN knowledge.

Other advantage of building the models in Excel or FORTRAN is that the working environment is Aspen Plus and therefore it is not necessary to export any model from one working environment to another, opposed to what happens when using Aspen Custom Modeller.



However, in terms of modifying the already existing model, ACM offers a work in progress environment with its platform especially designed for modelling and model development. Whenever the model is modified, the procedure is just to install it again in Aspen Plus, which is very simple. As far as Fortran and Excel are concerned regarding this aspect, there is also no problem in modifying the model, except when the model has already been converted into a custom form in the Model Library. In that case, the model has to be rebuilt and turned again into a custom form, follow all the procedures in VB.

## 6. Procedure

### 6.1. Software

The models and simulations were build and run in a computer with the characteristics and software versions shown in Tables 1 and 2.

**Table 1.** Computer characteristics

OS	Microsoft Windows XP Professional Version 2002 Service Pack 3
CPU	Intel® Pentium® 4 2.66 GHz
RAM	512 MB

**Table 2.** Software Versions

<i>Software</i>	<i>Version</i>
Net Visual Studio	MS VISUAL STUDIO .NET 2003
Compaq FORTRAN	Compaq Visual Fortran Professional Edition 6.5.0
Aspen Custom Modeler (ACM)	2004.1.13.2.0.0008
Aspen Plus	2004.1.13.2.4.3291

## 6.2. Solver settings in ACM and AP

In ACM as well as AP the default settings for the solver were not changed. This means that in both cases the solving method used was Newton, which will be briefly explained in the next paragraphs.

In addition to the default solver settings in ACM, homotopy was selected, because during modeling work it offered better convergence.

Newton method is an implementation of the modified Newton method for simultaneous nonlinear equations. Derivatives are calculated only when the rate of convergence is not satisfactory. The implementation allows bounds on the variables, and includes a line search for improved stability.

When using the Newton or Broyden methods to converge a flowsheet, a solution is found that minimizes the sum of squares of design specification and tears stream errors, divided by their tolerances. Iterations stop when the root mean square of the changes in the scaled manipulated variables is less than a set tolerance. Aspen Plus scales each manipulated variable, dividing it by the absolute value of the lower or upper limit, whichever is larger.

## 6.3. Implementation

In this section a step-by-step explanation is presented on the models that were built to perform the simulations that lead to the results presented in the next chapter. In this work, three different models were built which are described in the following sub-chapters.

### 6.3.1. Model 1

The first model is a simple model considering the mass balance in one block without any discretization as it is shown in Figure 15.

The assumptions made in this model are that:

- The total pressures in the retentate, permeate and feed are constant
- The transport mechanism is the Solution-Diffusion mechanism
- Permeability and permeance are independent of pressure
- The partial pressure of the component in the feed is the partial pressure before the membrane
- The partial pressure of the component in the permeate is the partial pressure after the membrane
- Perfect mixing in the permeate side is assumed
- There is no pressure drop from feed to retentate
- Temperatures are constant
- Volume is constant

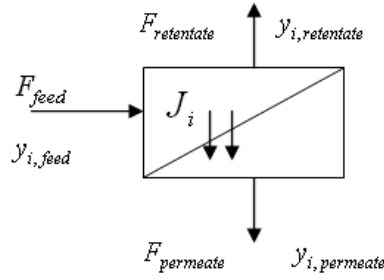


**Figure 15.** Schematic drawing of Model 1

The governing equations are:

$$F_{feed} = F_{permeate} + F_{retentate} \quad (21)$$

$$F_{feed} \cdot y_{i,feed} = F_{permeate} \cdot y_{i,permeate} + F_{retentate} \cdot y_{i,retentate} \quad (22)$$

$$J_i = \frac{F_{permeate} \cdot y_{i,permeate}}{A_{membrane}} \quad (23)$$

$$J_i = Q_i \cdot \left[ \frac{y_{i,feed} - y_{i,retentate}}{\ln\left(\frac{y_{i,feed}}{y_{i,retentate}}\right)} \cdot P_{feed} - y_{i,permeate} \cdot P_{permeate} \right] \quad (24)$$

The next figure shows the variables implemented in ACM that correspond to the equations 21-24. The description is available in the model's code in appendix 10.3.1.

The fixed variables correspond to the input given to the model that in this case are feed temperature, pressure and composition as well as retentate, permeate pressure, membrane area and permeances.

Name	Spec	Variable Type
GPU.A	Fixed	area
GPU.Inlet.F	Fixed	flow_mol
GPU.Inlet.P	Fixed	pressure
GPU.Inlet.T	Fixed	temperature
GPU.Inlet.z("CH4")	Fixed	molefraction
GPU.Inlet.z("CO2")	Fixed	molefraction
GPU.L("CH4")	Fixed	notype
GPU.L("CO2")	Fixed	notype
GPU.Permateate.P	Fixed	pressure

**Figure 16.** Input of Model 1 in ACM

### 6.3.2. Model 2

In this model the membrane module was broken down into  $k$  cells of equal length and each cell behaves like the simple model. Hence, for each cell the assumptions made for Model 1 apply. The number of cells is defined in the code and it is possible to change.

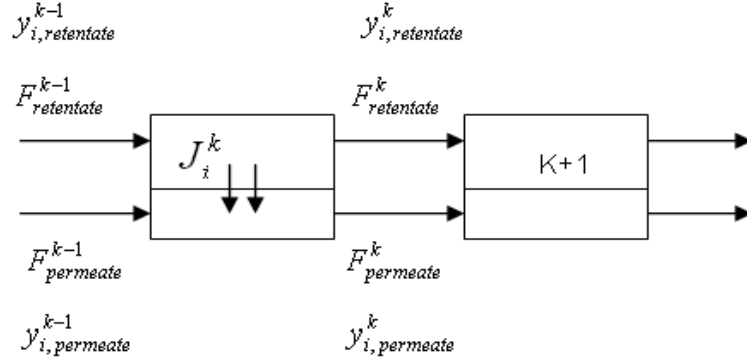


**Figure 17.** Schematic drawing of Model 2

$$F_{retentate}^{k-1} + F_{permeate}^{k-1} = F_{retentate}^k + F_{permeate}^k \quad (25)$$

$$F_{retentate}^{k-1} \cdot y_{i,retentate}^{k-1} + F_{permeate}^{k-1} \cdot y_{i,permeate}^{k-1} = F_{retentate}^k \cdot y_{i,retentate}^k + F_{permeate}^k \cdot y_{i,permeate}^k \quad (26)$$

$$J_i^k = \frac{F_{permeate}^k \cdot y_{i,permeate}^k}{A_k} \quad (27)$$

$$J_i^k = Q_i \cdot \left[ \frac{y_{i,retentate}^{k-1} - y_{i,retentate}^k}{\ln\left(\frac{y_{i,retentate}^{k-1}}{y_{i,retentate}^k}\right)} \cdot P_{feed} - y_{i,permeate}^k \cdot P_{permeate} \right] \quad (28)$$

The next figure shows the variables implemented in ACM that correspond to the equations 25-28. The description is available in the model's code in appendix 10.3.2.

The fixed variables correspond to the input given to the model that in this case are feed temperature, pressure and composition as well as retentate, permeate pressure, membrane area and permeances. The conditions for module  $k=0$  were also defined. The retentate conditions of  $k=0$  are the feed's conditions and for the permeate they equal zero.

Name	Spec	Description	Variable Type
GPU.A	Fixed	Total membrane area	area
GPU.FPerm(0)	Fixed	Permeate mole flow from cell	flow_mol
GPU.Inlet.F	Fixed	Molar flow rate	flow_mol
GPU.Inlet.P	Fixed	Pressure	pressure
GPU.Inlet.T	Fixed	Temperature	temperature
GPU.Inlet.z("CH4")	Fixed	Mole fractions	molefraction
GPU.Inlet.z("CO2")	Fixed	Mole fractions	molefraction
GPU.Lmol("CH4")	Fixed	Molar permeability (kmol/(m...	notype
GPU.Lmol("CO2")	Fixed	Molar permeability (kmol/(m...	notype
GPU.PPerm	Fixed	Permeate pressure	pressure
GPU.ZPerm("CH4",0)	Fixed	Permeate mole fraction in cell	molefraction
GPU.ZPerm("CO2",0)	Fixed	Permeate mole fraction in cell	molefraction

**Figure 18.** Input of Model 1 in ACM

### 6.3.3. Model 3

In this model the discretization tools of ACM were used to create yet another discretized model. Using this discretization method on which the partition of the membrane is implemented by ACM, the user only has to write in the code the differential equations of the model. It is also possible to change the node spacing so that certain parts of the membrane are divided into smaller parts than others, i.e. the discretization method, without changing the code of the model. In this model's case, since it is a simple model, such feature was not analyzed. However, the construction of a model on which the discretization is not implemented by the user is useful to confirm the results obtain with Model 2.

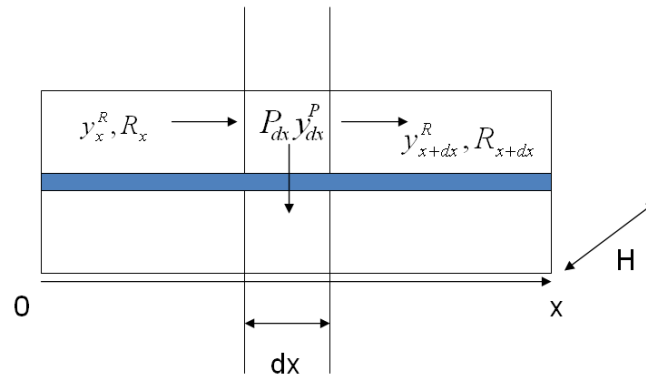


**Figure 19.** Schematic drawing of Model 3

For each component the following relations apply:

$$d(y_{(x)}^R \cdot R_{(x)}) = -Q \cdot (y_{(x)}^R \cdot p^R - y_{(x)}^P \cdot p^P) \cdot dA \quad (29)$$

$$d(y_{(x)}^P \cdot P_{(x)}) = Q \cdot (y_{(x)}^R \cdot p^R - y_{(x)}^P \cdot p^P) \cdot dA \quad (30)$$

$$dA = H \cdot dx \quad (31)$$

$$d(y_{(x)}^P \cdot P_{(x)}) = k \cdot (y_{(x)}^R \cdot p^R - y_{(x)}^P \cdot p^P) \cdot dx \quad (32)$$

$$k = H \cdot Q \quad (33)$$

The next figure shows the variables implemented in ACM that correspond to the equations 25-28. The description is available in the model's code in appendix 10.3.3.

The fixed variables correspond to the input given to the model that in this case are feed temperature, pressure and composition as well as permeate pressure, membrane area and the constant parameter k of equation 33. The conditions for module when  $x=0$  were also defined in the code. The retentate conditions of  $x=0$  are the feed's conditions and for the permeate they equal zero.

Name	Spec	Description	Variable Type
B1.Permeate.P	Fixed	Pressure	pressure
B1.k("CO2")	Fixed		constant
B1.k("CH4")	Fixed		constant
B1.Feed.z("CO2")	Fixed	Mole fractions	molefraction
B1.Feed.z("CH4")	Fixed	Mole fractions	molefraction
B1.Feed.P	Fixed	Pressure	pressure
B1.Feed.F	Fixed	Molar flow rate	flow_mol

**Figure 20.** Input of Model 3 in ACM

## 6.4. Setting up the components

The components in ACM can be defined as a list of components or a set of components, the difference with this work being that in the latter case the components have properties associated to them. In all the simulations performed in ACM within this work component sets were used.

To define the component set it is first necessary to generate an Aspen Property Definition File so that ACM can access that file for the properties. In order to generate that file it is necessary to run a Property Simulation with the desired components.

The model created is not bounded with these components, when importing the model to AP it is possible to change the components.

## 6.5. Writing the code

The model's equations, variables and parameters were written in the ACM reference language. Three distinct parts mainly compose the code. First, the variables and parameters are declared stating the name, the type and a brief description, which is optional but quite useful to keep track of the units. When using differential equations it is also necessary to define the domain and dimension of the variables.

```
/ Parameters and variables
NCells      as IntegerParameter (Description:"Number of cross flow cells", 100);
A           as Area              (Description:"Total membrane area", Fixed); // (m2)
L(ComponentList) as Notype       (Description:"Permeability in m3(STP)/(m2 h bar)", Fixed);
Lmol(ComponentList) as Notype    (Description:"Molar permeability (kmol/(m2 h bar))");
PPerm       as Pressure          (Description:"Permeate pressure", Fixed); // (bar)
ACell       as Area              (Description:"Area per cross flow cell (m2)");
FRet([0:NCells]) as Flow_Mol     (Description:"Retentate mole flow from cell"); // (kmol/h)
FPerm([0:NCells]) as Flow_Mol    (Description:"Permeate mole flow from cell"); // (kmol/h)
ZRet(ComponentList,[0:NCells]) as Molefraction (Description:"Retentate mole fraction in cell");
ZPerm(ComponentList,[0:NCells]) as Molefraction (Description:"Permeate mole fraction in cell");
Jmol(ComponentList,[1:NCells]) as Flow_Mol    (Description:"Permeate mole flux in cell");
RhoRet      as hidden Dens_Mol; // Retentate molar density (kmol/m3)
RhoPerm     as hidden Dens_Mol; // Permeate molar density (kmol/m3)
```

Figure 21. Variable definition In ACM

```
//dominio
x as LengthDomain (DiscretizationMethod:"BFD1", HighestOrderDerivative: 1, Length:10, SpacingPreference:1);

//distribuciao
Ret as Distribution1D (XDomain is X) of Flow_Mol;
Perm as Distribution1D (XDomain is X) of Flow_Mol;
k(ComponentList) as constant;
yret(ComponentList) as Distribution1D (XDomain is X) of Molefraction;
yperm(ComponentList) as Distribution1D (XDomain is X) of Molefraction;
```

Figure 22. Variable, domain and distribution definition in ACM



Since it is necessary for the model to have an input in the form of streams, it is necessary to link the inlet streams to the input of the model and the outlet streams to the output of the model. To do this, the inputs and the outputs are defined as “Ports”. These ports have defined base units and properties such as temperature, composition or pressure and therefore it is not necessary to declare them as variables in the first part of the code. The port type used in the models was MoleFraction Port and its variable types are resumed in Table 3. It is very important to define the constants of the model in the same units as the Ports’, because all the calculations are made in those units. After defining the variables and ports, the core of the model is built by inserting the model’s equations into the code. In the end the code is compiled and the degrees of freedom (DOF) are calculated. The codes for the models can be found in the Appendix 10.3.1 - 3.

**Table 3.** Port description and base units

Property	Code	Base Units
Molar flow rate	Flow_mol	kmol/hr
Mole fractions	Molefraction	kmol/kmol
Temperature	Temperature	C
Pressure	Pressure	bar
Molar volume	Vol_mol	m3/kmol
Molar enthalpy	Enth_mol	GJ/kmol

## 6.6. Building the icons

There is also the option of drawing icons for the model to be represented in the flowsheet. Figures 20, 21 and 22 represent the icons for model 1, 2 and 3, respectively. These icons are part of the model and are also exported to AP.

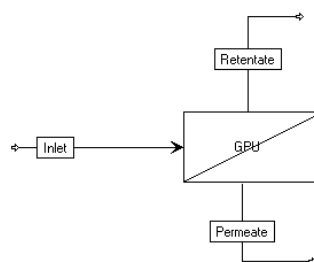


**Figure 23.** Schematic drawing of Model 1

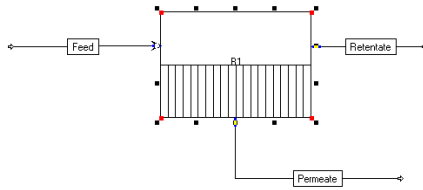


**Figure 24.** Schematic drawing of Model 2

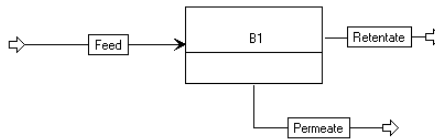


**Figure 25.** Schematic drawing of Model 3

## 6.7. Setting the variables

Since ACM runs in an equation-oriented environment, degrees of freedom (DOF) have to be taken into account. In order to have a solution for the system of equations, not only the number of variables that need to be fixed has to be the same as the system's DOF, but also the system has to be represented by a non-singular matrix.

In ACM it is possible to track if your equation set is solvable or not, because there is a specification editor that helps fixing the variables and gives the specification status for the model that is being built.

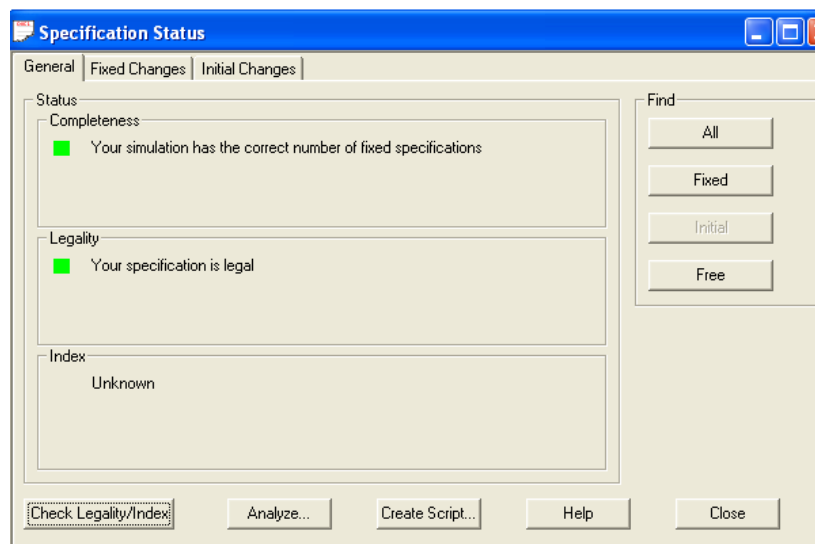


**Figure 26.** Specification Status window in ACM

In order for the models to be solvable the DOF must equal zero. The fixed variables are defined for each model, being the fixed variables inputs and constants and free variables calculated variables.

## **6.8. Exporting the model to Aspen Plus**

In order to export the model created in ACM to AP it is necessary to have installed, besides ACM and AP, a Microsoft C++ compiler.

To export the model:

- From the Exploring Simulation pane, right click on Simulations\Custom Modelling\Models\... and pick the Model Package Properties wizard. Explore the various options available through the wizard for configuring the install package and accept the default options as saved in \*.acmf.
- From the “Exploring Simulation” pane, right click on Simulations\Custom Modelling\Models\... and pick the .Export wizard, toggle the Save As Model Installation Package(\*.msi), pick a convenient directory and click the Save button.
- When Aspen Custom Modeller asks whether you want to install the package, hit “yes” and follow the installation instructions.
- Exit Aspen Custom Modeller.

The model has been exported to AP. In order to appear in the Model Library of Aspen Plus the model has to be selected in the References option of the Library menu of AP. After this the option ACM Models has to be selected.

## 6.9. Simulation environment in Aspen Plus

When the model is exported and placed in the model library as explained before, it behaves like a normal block in AP. The block options are present on a table like in the EO environment of AP, but the block can be solved using the sequential modular settings like any other model from the model library.

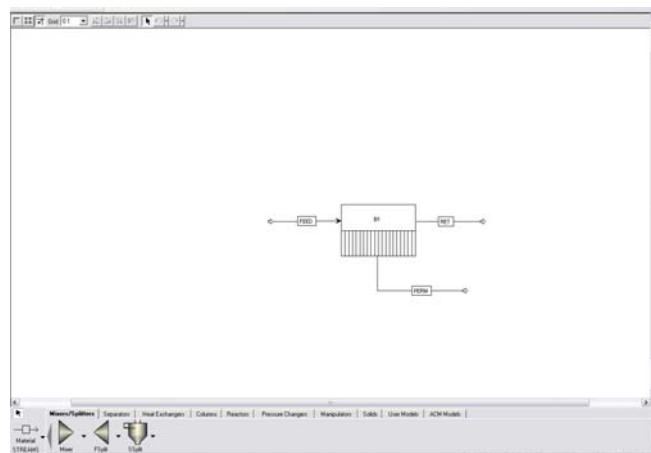


Figure 27. Model 2 in AP simulation environment

Index	Variable	Value	Units	Physical Type	Connection Type	Specification	Lower Bound	Upper Bound	Step Bound	Initial Value	Change	Internal
1	A	20		AREA	Constant	Constant	0	1e+006	1e+035	1e+035	-1e+035	1
2	UNIFIED	1	*	UNIFIED	UNIFIED	Calculated	-1e+030	1e+030	1e+035	1e+035	-1e+035	1
3	UNIFIED	1	*	UNIFIED	UNIFIED	Calculated	-1e+030	1e+030	1e+035	1e+035	-1e+035	1
4	UNIFIED	0.00115	*	UNIFIED	UNIFIED	Constant	-1e+030	1e+030	1e+035	1e+035	-1e+035	1
5	UNIFIED	0.00368	*	UNIFIED	UNIFIED	Constant	-1e+030	1e+030	1e+035	1e+035	-1e+035	1
6	PRESSURE	1	BAR	PRESSURE	PRESSURE	Constant	-1e+030	1e+030	1e+035	1e+035	-1e+035	1
7	AREA	1	AREA	AREA	AREA	Calculated	0	1e+006	1e+035	1e+035	-1e+035	1
8	PRET(1)	10	KMOL/H	MOLE-FLOW	MOLE-FLOW	Calculated	0	1e+010	1e+035	1e+035	-1e+035	1
9	PRET(1)	10	KMOL/H	MOLE-FLOW	MOLE-FLOW	Calculated	0	1e+010	1e+035	1e+035	-1e+035	1
10	PRET(2)	10	KMOL/H	MOLE-FLOW	MOLE-FLOW	Calculated	0	1e+010	1e+035	1e+035	-1e+035	1
11	PRET(3)	10	KMOL/H	MOLE-FLOW	MOLE-FLOW	Calculated	0	1e+010	1e+035	1e+035	-1e+035	1
12	PRET(4)	10	KMOL/H	MOLE-FLOW	MOLE-FLOW	Calculated	0	1e+010	1e+035	1e+035	-1e+035	1
13	PRET(5)	10	KMOL/H	MOLE-FLOW	MOLE-FLOW	Calculated	0	1e+010	1e+035	1e+035	-1e+035	1
14	PRET(6)	10	KMOL/H	MOLE-FLOW	MOLE-FLOW	Calculated	0	1e+010	1e+035	1e+035	-1e+035	1
15	PRET(7)	10	KMOL/H	MOLE-FLOW	MOLE-FLOW	Calculated	0	1e+010	1e+035	1e+035	-1e+035	1
16	PRET(8)	10	KMOL/H	MOLE-FLOW	MOLE-FLOW	Calculated	0	1e+010	1e+035	1e+035	-1e+035	1
17	PRET(9)	10	KMOL/H	MOLE-FLOW	MOLE-FLOW	Calculated	0	1e+010	1e+035	1e+035	-1e+035	1
18	PRET(10)	10	KMOL/H	MOLE-FLOW	MOLE-FLOW	Calculated	0	1e+010	1e+035	1e+035	-1e+035	1
19	PRET(11)	10	KMOL/H	MOLE-FLOW	MOLE-FLOW	Calculated	0	1e+010	1e+035	1e+035	-1e+035	1
20	PRET(12)	10	KMOL/H	MOLE-FLOW	MOLE-FLOW	Calculated	0	1e+010	1e+035	1e+035	-1e+035	1
21	PRET(13)	10	KMOL/H	MOLE-FLOW	MOLE-FLOW	Calculated	0	1e+010	1e+035	1e+035	-1e+035	1
22	PRET(14)	10	KMOL/H	MOLE-FLOW	MOLE-FLOW	Calculated	0	1e+010	1e+035	1e+035	-1e+035	1
23	PRET(15)	10	KMOL/H	MOLE-FLOW	MOLE-FLOW	Calculated	0	1e+010	1e+035	1e+035	-1e+035	1
24	PRET(16)	10	KMOL/H	MOLE-FLOW	MOLE-FLOW	Calculated	0	1e+010	1e+035	1e+035	-1e+035	1
25	PRET(17)	10	KMOL/H	MOLE-FLOW	MOLE-FLOW	Calculated	0	1e+010	1e+035	1e+035	-1e+035	1
26	PRET(18)	10	KMOL/H	MOLE-FLOW	MOLE-FLOW	Calculated	0	1e+010	1e+035	1e+035	-1e+035	1
27	PRET(19)	10	KMOL/H	MOLE-FLOW	MOLE-FLOW	Calculated	0	1e+010	1e+035	1e+035	-1e+035	1
28	PRET(20)	10	KMOL/H	MOLE-FLOW	MOLE-FLOW	Calculated	0	1e+010	1e+035	1e+035	-1e+035	1
29	PRET(21)	10	KMOL/H	MOLE-FLOW	MOLE-FLOW	Calculated	0	1e+010	1e+035	1e+035	-1e+035	1
30	PRET(22)	10	KMOL/H	MOLE-FLOW	MOLE-FLOW	Calculated	0	1e+010	1e+035	1e+035	-1e+035	1
31	PRET(23)	10	KMOL/H	MOLE-FLOW	MOLE-FLOW	Calculated	0	1e+010	1e+035	1e+035	-1e+035	1
32	PRET(24)	10	KMOL/H	MOLE-FLOW	MOLE-FLOW	Calculated	0	1e+010	1e+035	1e+035	-1e+035	1
33	PRET(25)	10	KMOL/H	MOLE-FLOW	MOLE-FLOW	Calculated	0	1e+010	1e+035	1e+035	-1e+035	1
34	PRET(26)	10	KMOL/H	MOLE-FLOW	MOLE-FLOW	Calculated	0	1e+010	1e+035	1e+035	-1e+035	1
35	PRET(27)	10	KMOL/H	MOLE-FLOW	MOLE-FLOW	Calculated	0	1e+010	1e+035	1e+035	-1e+035	1
36	PRET(28)	10	KMOL/H	MOLE-FLOW	MOLE-FLOW	Calculated	0	1e+010	1e+035	1e+035	-1e+035	1
37	PRET(29)	10	KMOL/H	MOLE-FLOW	MOLE-FLOW	Calculated	0	1e+010	1e+035	1e+035	-1e+035	1
38	PRET(30)	10	KMOL/H	MOLE-FLOW	MOLE-FLOW	Calculated	0	1e+010	1e+035	1e+035	-1e+035	1

Figure 28. Block options of ACM model exported to AP in AP simulation environment

The model block can be linked via streams with all the other blocks and all operations are possible. However, since any heat streams are specified in the model, it only supports material streams.

## 7. Results

In the next subchapters the main results of the AP simulations done with the models built in ACM, which were described before, are shown.

Firstly, the main results of the validation of each model results with experimental data are presented for the methane/carbon dioxide mixture. Then, the output of each model is compared with each other and one is chosen to perform the sensitivity analysis for the separation of hydrogen/carbon dioxide mixture.

### 7.1. Experimental Validation

The experimental data used to compare the model's results with a real system are taken from [18]. The module used to obtain the experimental data was a hollow fibre module. The experimental setting of the module as well as membrane parameters can be found in Figure 29 and Table 4, respectively.

For each model three sets of experimental data are compared. Firstly, permeate flow vs. feed flow, retentate flow vs. feed flow and finally retentate composition vs. feed flow.

The first two were compared mostly to conclude which of the models offered better results regarding the way the permeation was described in terms of total permeation through the membrane. Since the membrane from the experimental set-up was a reverse-selective membrane the composition in the retentate, in terms of methane, concentration is analyzed.

In order to calculate the permeances, the flow through the membrane of the experimental set-up of each pure component separately was studied. The pressure of the feed was increased and the pressure of the permeate and rate were measured. To calculate an average permeance for the pure components to use in the models, equations 17 and 18 were used for each point of the experimental data and then an average was calculated. The permeances calculated can be found in Table 4 and as well as the membrane's characteristics.

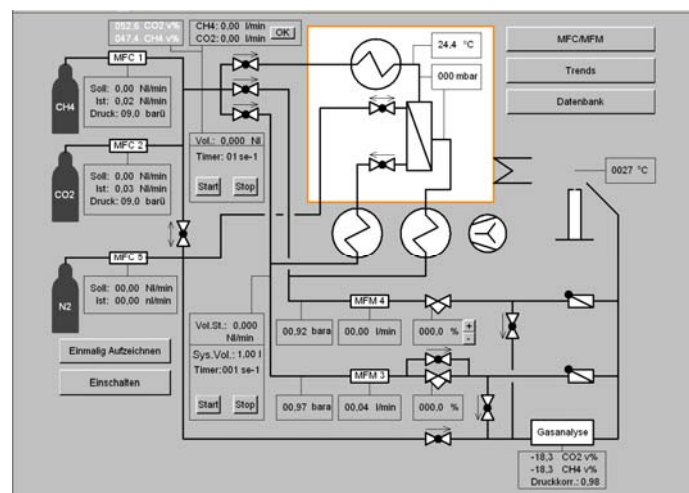


**Figure 29.** Experimental set-up of the membrane used in the validation

**Table 4.** Membrane properties and component permeances

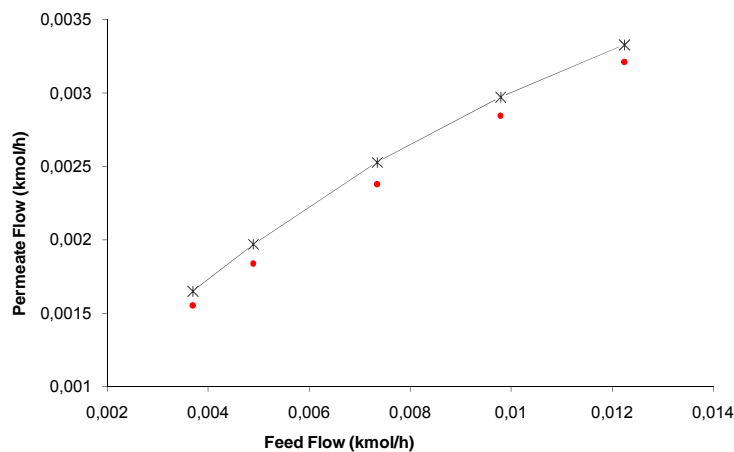
Number of fibers	800
Length (m)	0,38
Di (mm)	0,40
At (m <sup>2</sup> )	0,38
Q(CH <sub>4</sub> ) (kmol/h.bar.m <sup>2</sup> )	2,00x10 <sup>-4</sup>
Q(CO <sub>2</sub> ) (kmol/h.bar.m <sup>2</sup> )	8,27x10 <sup>-3</sup>

The results for the discretized models were obtained using 100 modules and 100 nodes of Models 2 and 3, respectively.

#### 7.1.1. Model 1

Figures 30 e 31 represent, respectively, the permeate flow and retentate flow obtained when the feed flow was varied from  $3,70 \times 10^{-3}$  to  $12,24 \times 10^{-3}$  kmol/h. The experimental data is represented by the points.

The feed composition in the experiment varied slightly from 64,88% to 65,01% but in the model a constant feed composition of 65% of CH<sub>4</sub> and 35% CO<sub>2</sub> was assumed. The maximum deviation obtained with this model to the experimental that was an increase of 7,06 % in the permeate flow and 4,55% in the retentate flow.

**Figure 30.** Permeate flow vs. Feed Flow obtained with Model 1 and experimental data

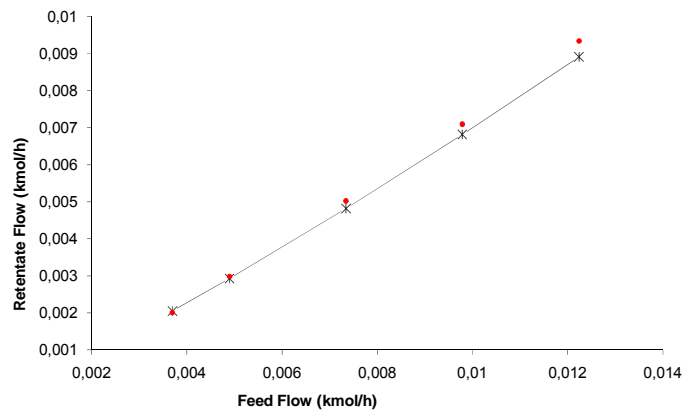


**Figure 31.** Retentate flow vs. Feed Flow obtained with Model 1 and experimental data

The next plot shows the model's output compared with experimental results for the methane concentration in the retentate. The trend obtained with the model in this case is different from the experimental data's trend originating, for low feed rates, the maximum deviation to the experimental data of 3,42% increase in methane concentration.

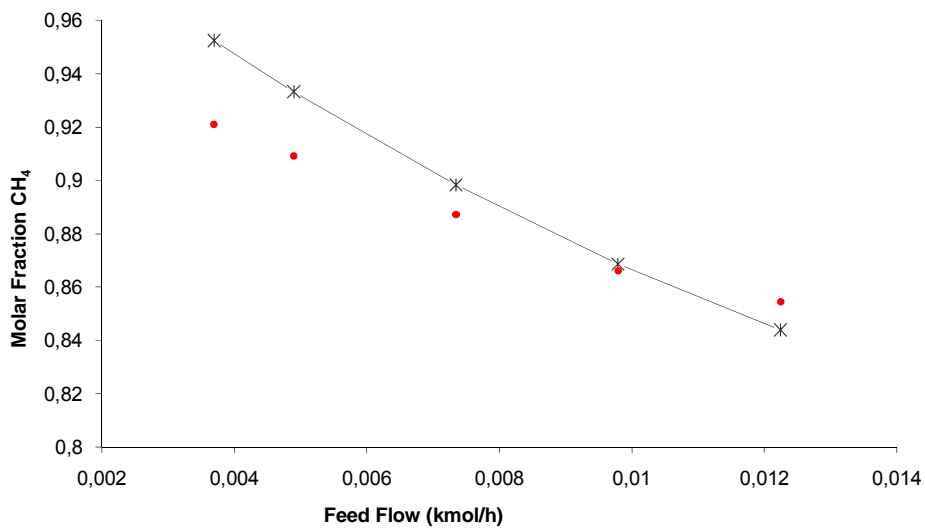


**Figure 32.** Methane concentration vs. Feed Flow obtained with Model 1 and experimental data

### 7.1.2. Model 2

With model 2 the results obtained were less deviated from the experimental data that the model presented before. The maximum deviation obtained with this model to the experimental that was an increase of 1,14 % in the permeate flow and an increase of 5,77% in the retentate flow. However, in this model, the trend obtained by the model's output follows the trend given by the experimental data

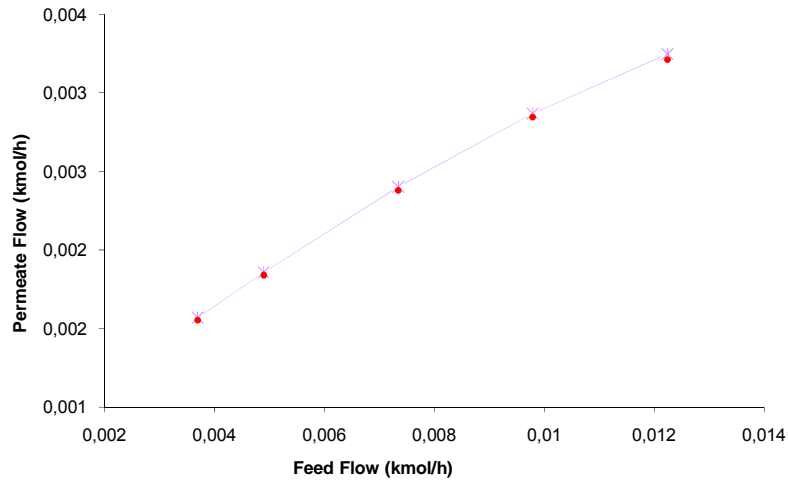


**Figure 33.** Permeate flow vs. Feed Flow obtained with Model 2 and experimental data

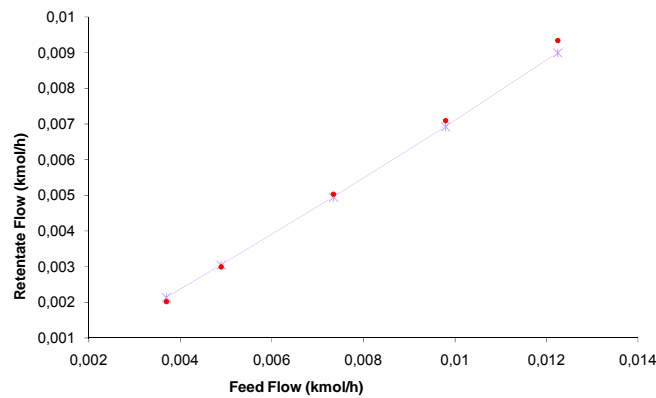


**Figure 34.** Retentate flow vs. Feed Flow obtained with Model 2 and experimental data



As far as the model's output for the concentration of methane in the retentate is concerned, the values of the experimental data are slightly higher than the ones calculated by the model. The largest deviation between the model's concentration and the experimental data's is a decrease of 2,61%

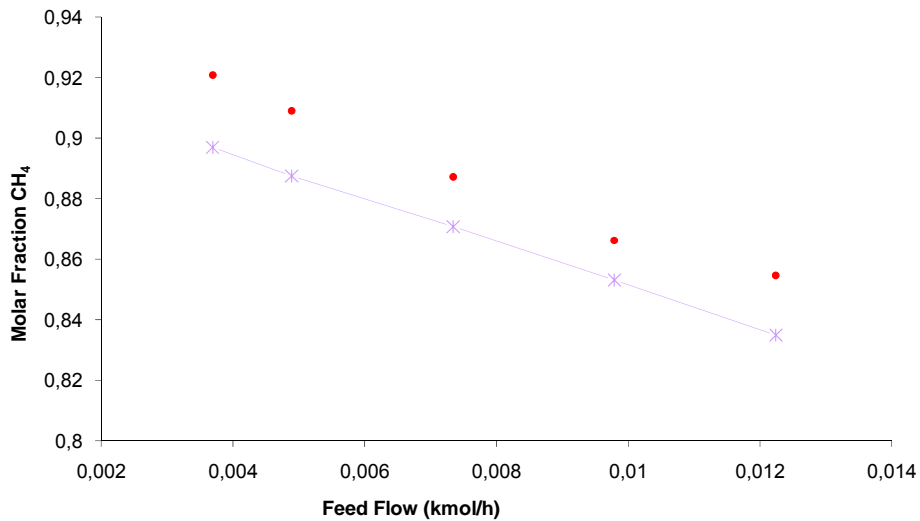


**Figure 35.** Methane concentration vs. Feed Flow obtained with Model 2 and experimental data

### 7.1.3. Model 3

The results for the third model are similar with the results of the previous model. Similarly, the results obtained were less deviated from the experimental data than the results of model 1. As far as the values for permeate flow obtained using simulation the maximum deviation observed was an increase of 0,56% and in the retentate flow an increase of 6,44%. In both cases the trends obtained by the models' output follows the trend given by the experimental data

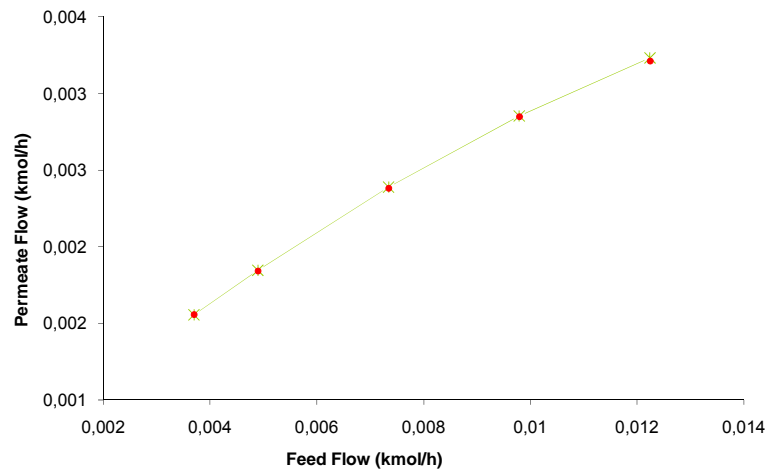


**Figure 36.** Permeate flow vs. Feed Flow obtained with Model 3 and experimental data

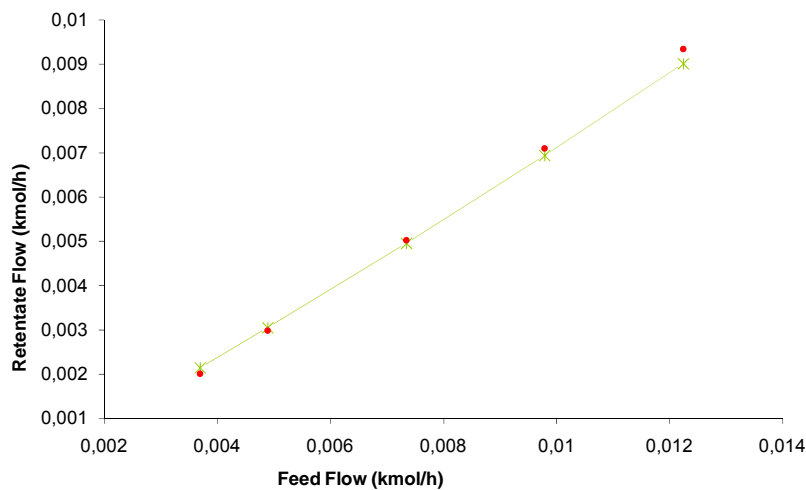


**Figure 37.** Retentate flow vs. Feed Flow obtained with Model 3 and experimental data

The next plot shows the model's results compared with experimental results for the methane concentration in the retentate. The maximum deviation to the experimental data is a decrease in methane concentration by 2,71%.

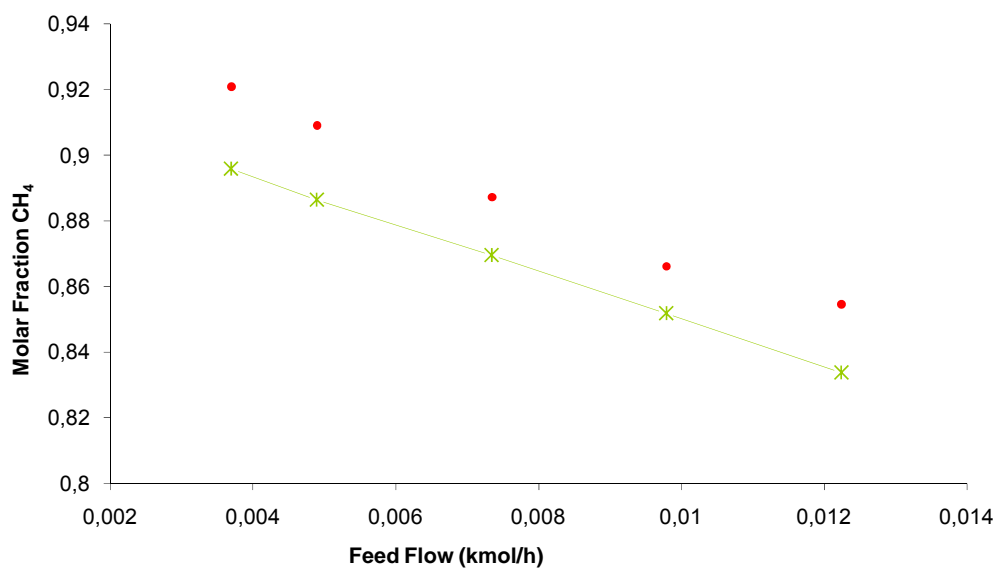


**Figure 38.** Methane concentration vs. Feed Flow obtained with Model 3 and experimental data

## 7.2. Comparison between the models

Concerning the permeate flow the model that has the closest results to the experimental data is Model 3, followed by Model 2 which presents similar results.

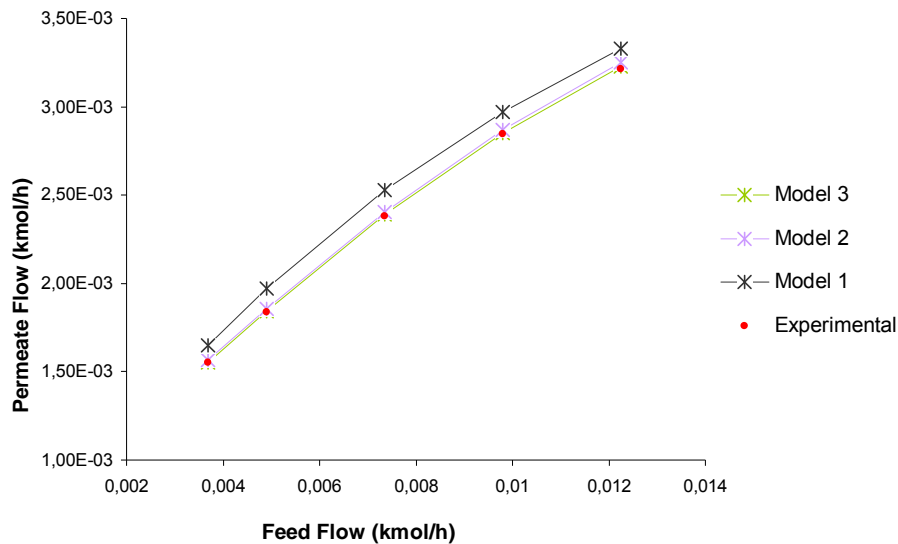


**Figure 39.** Comparison between models for the results of permeate flow vs. feed flow

The same happens with the results for the retentate flow. Model 3 presents the most approximate results to the experimental data, followed by Model 2, but in general, all 3 models give almost similar results.

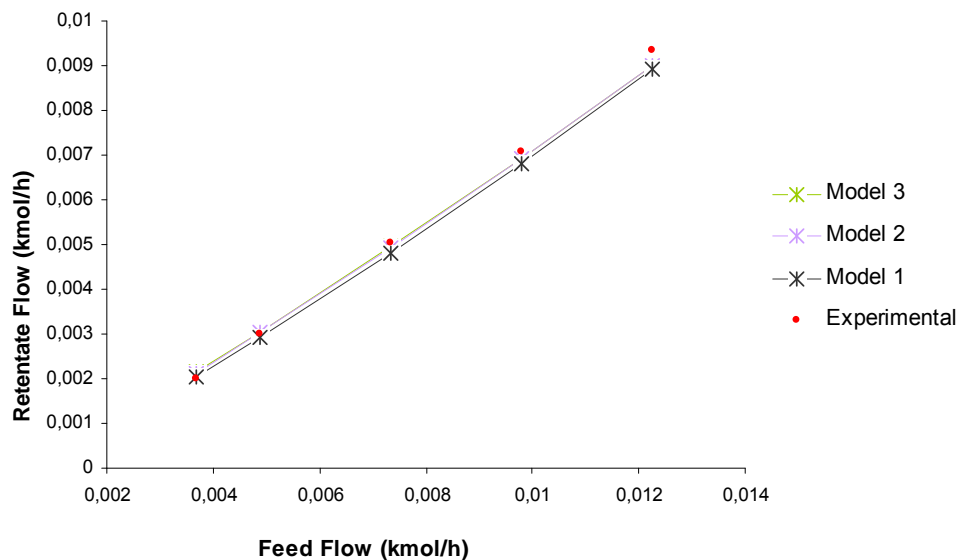


**Figure 40.** Comparison between models for the results of retentate flow vs. feed flow

As far as the concentration of methane in the retentate is concerned, both discretized model present the same results and follow the same trend as the experimental results. Only Model 1 gives a different trend as shown in Fig. 41.

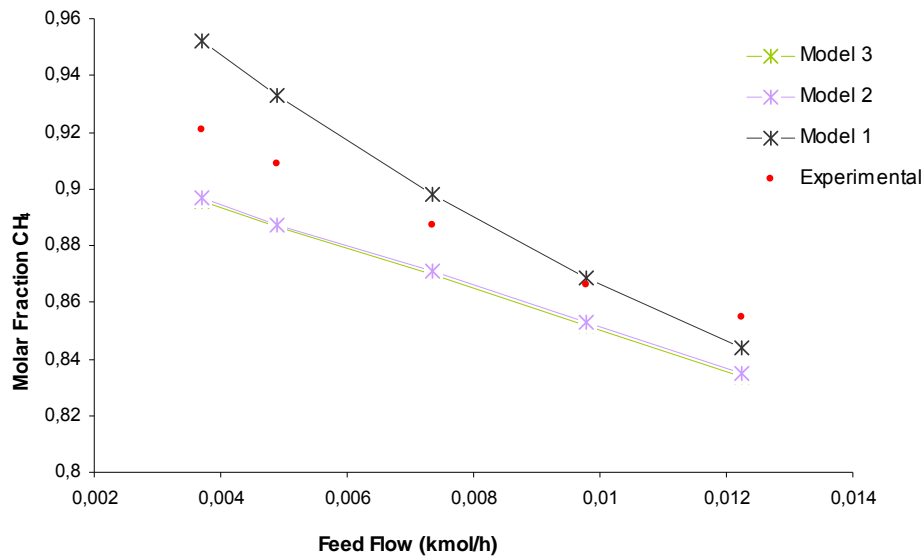


**Figure 41.** Comparison between models for the results of methane concentration vs. feed flow

The immediate conclusion one can take from the plots above is that discretization of the models fits better to the experimental data than a simple model without discretization. Moreover, one can also notice that from Model 1 to Model 3 the error in the calculated values for the retentate flow increase but the errors on the calculated permeate flow and methane concentration decrease.

The possible reason for the fact that the discretized models offer in general better results might have to do with convergence of the models. For instance, when dividing the membrane into smaller parts that means the equations described before are applied to each “slice” of the membrane taking into account that, for instance, closer to the feed side of the membrane the flux to the permeate is higher due to the bigger difference in the partial pressures of the components. This phenomenon is not accounted for when considering the membrane as a whole and even the approximation of calculating the logarithmic average of the partial pressure in the retentate side doesn’t offer as good results as the discretization of the module.

### 7.3. Sensitivity Analysis - Hydrogen recovery and molar fraction in retentate vs. membrane area

The final step in the calculations of this thesis was to choose a membrane and then perform sensitivity calculations for the mixture of hydrogen and carbon dioxide. The membrane that was chosen for these sensitivity analysis calculations was a PDMS membrane with the characteristics shown in the following table.

The main results analyzed are the carbon dioxide removed from the feed vs. the hydrogen lost to the permeate when the membrane's area increases and also the pressure of the permeate. Since hydrogen is the main product it is important to study the better way to retrieve the hydrogen present in the feed using the smallest area and lower energy consumption possible. In this sensitivity analysis only calculations for a single module are performed. The economic optimization of the membrane module is far from the scope of this thesis work but some initial conclusions on that topic can be taken with this simple analysis.

The model that was used to calculate the next results was model 2. Model 3 and model 2 presented similar results in the validation with experimental data and with the smallest deviations. However, to perform the calculations for the sensitivity analysis model 2 was chosen because the way it was implemented made it easier to change parameters and it is not necessary to specify the membrane's length.

**Table 5.** Membrane parameters

Permeability (Barrer)	3200 (CO <sub>2</sub> ) 950 (H <sub>2</sub> )
Thickness	1,3 µm

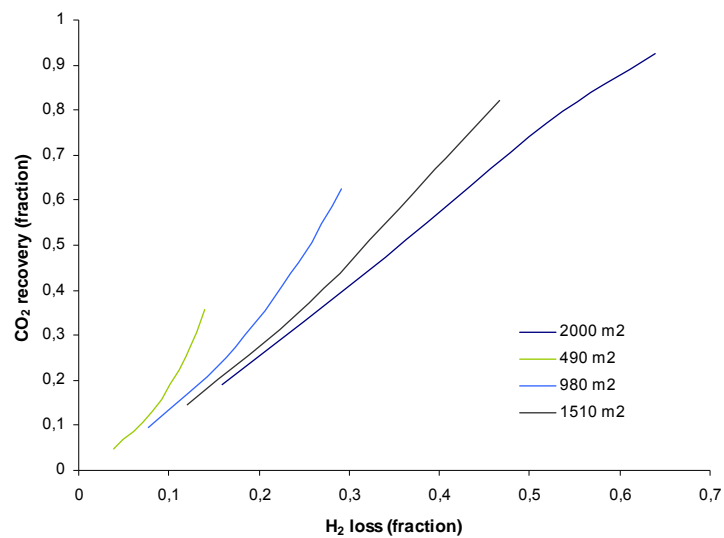
The reason this membrane was chosen to perform the sensitivity analysis was because it is an example of a polymeric membrane that is reverse selective at low temperatures and has been used in the separations of hydrogen and carbon dioxide. Since this membrane has a good permeability but a somewhat poor selectivity it is expected that to attain high concentrations of hydrogen in the retentate there will have to be loss to the permeate as well and vice versa.

Figure 42 and 43 represent the plots obtained by varying the membrane's area from 20 to 2000 m<sup>2</sup> and the permeate pressure from 0,7 to 6 bar, respectively, under feed conditions and process parameters presented in Table 6.

**Table 6.** Feed composition and operating conditions

Feed (kmol/h)	23,3
CO <sub>2</sub> mole fraction	0,3
H <sub>2</sub> mole fraction	0,7
Temperature (C)	35
Pressure (bar)	7,7

The next plot represents the trend of hydrogen loss to permeate and carbon dioxide recovery from feed when fixing the area and varying the permeate pressure. With increasing area and pressure the carbon dioxide recovery is higher but also the hydrogen loss to permeate.



**Figure 42.** CO<sub>2</sub> recovery vs H<sub>2</sub> loss to permeate for fixed areas increasing the pressure of permeate

The next plot once again represents the trend of hydrogen loss to permeate and carbon dioxide recovery from feed when fixing the pressure and varying the membrane area. With increasing area and pressure the

carbon dioxide recovery is higher but also the hydrogen loss to permeate, as it was observed before in Figure 42.

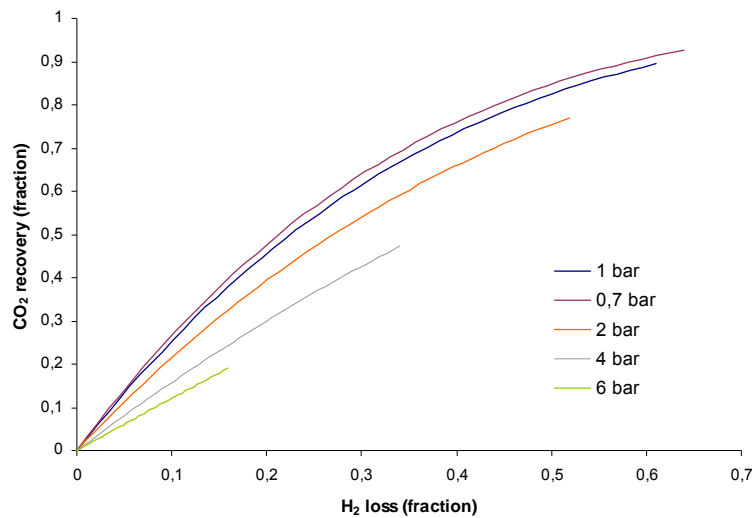


**Figure 43.** CO<sub>2</sub> recovery vs H<sub>2</sub> loss to permeate for fixed permeate pressures and increasing area

Figures 42 and 43 were combined in one plot that illustrates the parameters analyzed before but having the lines of constant pressure and constant area represented in one plot only, allows pinpointing the loss

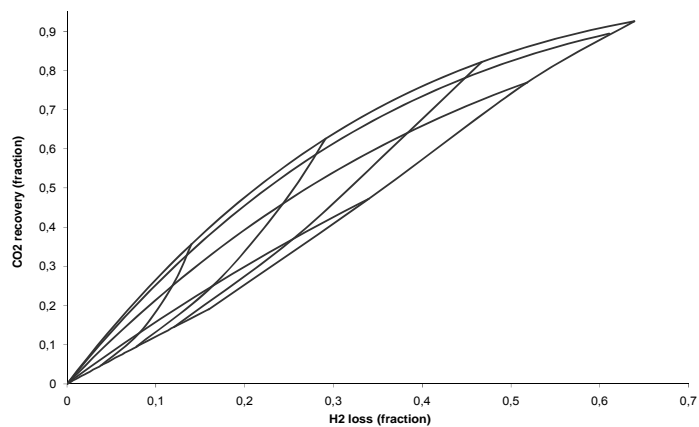


**Figure 44.** CO<sub>2</sub> recovery vs H<sub>2</sub> loss to permeate



As it was expected for this membrane, with increasing membrane area a higher concentration of hydrogen was calculated in the permeate. However with this increase in the concentration an increase in hydrogen loss to the permeate was also obtained. The same was observed when the permeate pressure was decreased, increasing the partial pressure difference between retentate and permeate.

A way to overcome the loss of hydrogen to the permeate would be to recycle the permeate and/or add another modules to the separation scheme.

Moreover, taking into account the deviations of this model, values for the concentration of the species in retentate are likely to be smaller than what it would be really possible to achieve with this type of membranes.

In this membrane's case when, for instance, a concentration higher than 0,8 is desired it means that the membrane area has to be higher than 1500 m<sup>2</sup> and the loss of hydrogen to the permeate will always be higher than 0,45.

## 8. Summary and Conclusions

The goal of this work was to develop a membrane gas permeation unit for the separation of Hydrogen and Carbon Dioxide. In order to achieve that goal it was necessary, first of all, to define which transport mechanism should be modelled and which type of membrane system should be used. Since there were still no real systems for the separation of the bio-hydrogen because the process is still in project phase, the main concept was to find a way to build a general model that could be improved later on with the development of the project. Therefore a single module using the solution-diffusion as a transport mechanism was developed which didn't consider the effects from temperature gradients, pressure drop or membrane's geometry. However, three different ways of describing the membrane module were considered, giving origin to three different models based on different ways to describe the flow, with or without discretization of the membrane module.

After this step came the selection of the software. The premise was that the models should run in AP and with that in mind some options like developing the model with the AP user models in connection with Excel or Fortran were studied. In the end the models were developed in ACM not only because it was already being used in the project but also because it presented itself to have the versatility needed.

During the work of this master thesis, three major bottleneck points were encountered. The first one during the installation of all the components necessary for the models built in ACM needed to be exported to AP. The second when learning the modelling language of ACM and finally the exportation of the model built to AP. Overcoming these three different phases made the progress of the work possible and had as an output the three models described above, the calculations to validate the model's results with experimental data as well as the sensitivity analysis presented before.

The models needed to be tested somehow before any calculation was done for the separation of gas mixtures of hydrogen and carbon dioxide. However experimental data for this separation was not available, therefore experimental results for the mixture methane and carbon dioxide were used. The premise taken was that if the validation for this mixture worked these models can also be used for the separation of hydrogen and carbon dioxide.

The first conclusion one takes immediately is that the results of the validation can be divided in two sets, the results of the discretized models 2 and 3 and the results of model 1. In both models 2 and 3 the results are very similar and closer to the experimental data which suggests that dividing the membrane into smaller parts describes the system more accurately. However, there seems to be a tendency of the models' methane concentration to have smaller values than those of the experimental data. This suggests that in the real system there is a phenomenon that promotes the permeation of carbon dioxide or "blocks" the permeation of methane through the membrane. Since the total flows of the retentate and permeate are almost the same in the models and in the experimental data, one is led to support a combination of both hypotheses as well as errors in permeance input of the models.

This additional permeation and blockage might have to do with all the factors that were disregarded such as temperature gradients or geometry. In addition to this, it is also necessary to notice that in the experimental setup, the flow was measured with standard volume units and that alone introduces an error on the reading of the flow and perhaps that is what causes such small differences between the models' output for total retentate and permeate flows to experimental data.

All in all, both models 2 and 3 seem to be able to predict quite well i.e. with a small error, the outcome of a gas permeation membrane unit and, for estimation purposes in a process, these models are suitable to be used. However, the ideal case would be that in the future corrections and alteration to this model can be made, perhaps even create a sort of a library within the model itself that allows the model user to choose which features in transport or geometry he/she wants in the system. Another upgrade that can be made is to add to the model the features necessary for dynamic simulation.

Nevertheless, it is crucial that validation with experimental data of the model can be made. Setting up a model for a membrane unit for software like AP should be a compromise between experimental work and computational work in order not only to troubleshoot but also to improve the results.

## 9. Literature

- [1] P.A.M. Claassen, T. de Vrije, R. Grabarczyk and K. Urbaniec, Congress CHISA 2006, Prague, Czech Republic, 2006
- [2] P.A.M. Claassen, T. de Vrije, M.A.V. Budde, 2nd World Conference on Biomass for Energy, Industry and Climate Protection, Rome, Italy, 2006
- [3] H.P. Goorissen and A.J.M. Stam, Proceedings of the 16th World Hydrogen Energy Conference, Lyon, France, 2006.
- [4] H., Koku, I. Eroglu, U.Gündüz, M. Yücel and L. Türker, Int. J. Hydrogen Energy 27 (2002) 1315.
- [5] E.W.J. van Niel, M.A.W. Budde, G.G. de Haas, F.J. van der Wal, P.A.M. Claassen, and A.J.M. Stam, Int. J. Hydrogen Energy 27 (2002) 1391.
- [6] W. Wukovits, A. Friedl, M. Schumacher, M. Modigell, K. Urbaniec, M. Ljunggren, G. Zacchi, P.A.M. Claassen, 15<sup>th</sup> European Biomass Conference & Exhibition, Berlin, Germany, 2007
- [7] W. Wukovits, Modarresi, A. Friedl., Conference PRES08, Prague, Czech.Rep., 2008
- [8] Wijmans J.G., Baker R.W., (1995), J. Membrane Sci., 107, 1-21
- [9] Mulder, M.: *Basic Principles of Membrane Technology*, Kluwer Academic Publishers, 2000, Dordrecht.
- [10] L. Shao, B.T. Low, T.-S. Chung, A.R. Greenberg, Polymeric Membranes for the Hydrogen Economy: Contemporary Approaches, Prospects for the Future, Journal of Membrane Science (2008)
- [11] S. Adhikari and S. Fernando, Hydrogen Membrane Separation Techniques, Ind. Eng. Chem. Res., Vol. 45, No. 3, 2006
- [12] ASPEN Plus Manual “Getting Started Customizing Unit Operation Models” Version 2004.1, AspenTech, 2005
- [13] ASPEN Plus Manual “User Models” Version 2004.1, AspenTech, 2005
- [14] Aspen Custom Modeler “Examples Guide”, Version 2004.1, AspenTech, 2005
- [15] Aspen Custom Modeler “Getting Started Guide”, Version 2004.1, AspenTech, 2005
- [16] Davis R. A., *Simple Gas Permeation and Pervaporation Membrane Unit Operation Models for Process Simulators*, Chem. Eng. Technol. 25 (2002), 7

- [17] Ohlrogge K., Ebert K., *Membranen: Grundlagen, Verfahren und industrielle Anwendungen*, Wiley-VCH, 2006
- [18] Alekssander Makaruk, Internal publication
- [19] H. Lin and B.D. Freeman, Gas solubility, diffusivity and permeability in poly(ethylene oxide), *J. Membr. Sci.* **239** (2004), pp. 105–117
- [20] M. Yoshino, K. Ito, H. Kita and K.I. Okamoto, Effects of hard-segment polymers on CO<sub>2</sub>/N<sub>2</sub> gas-separation properties of poly(ethylene oxide)-segmented copolymers, *J. Polym. Sci. B: Polym. Phys.* **38** (2000), pp. 1707–1715.
- [21] K. Okamoto, M. Fujii, S. Okamoto, H. Suzuki, K. Tanaka and H. Kita, Gas permeation properties of poly(ether imide) segmented copolymers, *Macromolecules* **28** (1995), pp. 6950–6956.
- [22] H. Suzuki, K. Tanaka, H. Kita, K. Okamoto, H. Hoshino and T. Yshinaga, Preparation of composite hollow fiber membranes of poly(ethylene oxide)-containing polyimide and their CO<sub>2</sub>/N<sub>2</sub> separation properties, *J. Membr. Sci.* **146** (1998), pp. 31–37.
- [23] Y. Yin, L.M. Yang, M. Yoshino, J.H. Fang, K. Tanaka and H. Kita, Synthesis and gas permeation properties of star-like poly(ethylene oxide)s using hyperbranched polyimide as central core, *Polym. J.* **36** (2004), pp. 294–302.
- [24] I. Blume, I. Pinnau, Composite membrane, method of preparation and use, US Patent No. 4,963,165 (1990).
- [25] V.I. Bondar, B.D. Freeman and I. Pinnau, Gas transport properties of poly(ether-b-amide) segmented block copolymers, *J. Polym. Sci. B: Polym. Phys.* **38** (2000), pp. 2051–2062.
- [26] J.W. Simmons, Block polyurethane-ether and polyurea-ester gas separation membranes, US Patent No. 6,843,829 (2005).
- [27] J.W. Simmons, Block polyester-ether gas separation membranes, US Patent No. 6,860,920 (2005).
- [28] A. Morisato and I. Pinnau, Synthesis and gas permeation properties of poly(4-methyl-2-pentyne), *J. Membr. Sci.* **121** (1996), pp. 243–250.

## 10. Appendix

## 10.1. Troubleshooting the export of an ACM model to AP

1. Install AP + ACM
2. Install C++ compiler and Fortran
3. Open the tutorial file on how to export an ACM model to AP
4. Follow the procedure
5. If the export fail due to “-nmake file error” this means the compilers are not well installed
6. Check the computer's system variables and verify if the compilers folder are configured in BIN, PATH and INCLUDE
7. If so, try to uninstall AP, ACM and the compiler and install everything again, this time installing the compilers first
8. Repeat 3 and 4
9. If error 5 still exists, repeat 6.
10. If it continues to fail it means that the system's files are corrupted
11. Try to change/add the files
12. If everything else fails, format and repeat 1. to 4.

## 10.2. Tips on using ACM

1. When writing the model's code avoid divisions and logarithms
2. Use the appropriate units so that there aren't too big or too small numbers otherwise the system may not converge
3. Always define the order of magnitude of the variables for the same reasons of 2.
4. Not every model with a full specification can be solved
5. Identify the equations
6. Not every port type can be exported to AP
7. Keep it simple



## 10.3. Models' Source Codes

### 10.3.1. Model 1

```
A                as Area                (Description:"Total membrane area"); // (m2)
Jmol(ComponentList) as Flow_Mol        (Description:"Molar Flux through the membrane/(kmol/h)");
J(ComponentList)   as Flow_Vol        (Description:"Molar Flux through the membrane/(m3(STP)/h)");
Ppav(ComponentList) as Pressure        (Description:"Permeate average pressure"); // (kPa)
Pfav(ComponentList) as Pressure        (Description:"Feed average pressure"); // (kPa)
K(ComponentList)   as Notype           (Description:"Constant");

// Ports
Inlet    as Input  MoleFractionPort;
Retentate as Output MoleFractionPort;
Permeate  as Output MoleFractionPort;

// Convert flux to molar basis
J = (Jmol * (273.15*0.314))/101.325;

// Other outlet stream conditions
Retentate.T = Inlet.T;
Permeate.T  = Inlet.T;

// Equations
GlobalMass:      Inlet.F = Retentate.F + Permeate.F;
PermeateFlow:    Permeate.F = sigma (foreach (comp in componentlist) Jmol(comp));
Permeate.P = sigma (foreach (comp in componentlist) Ppav(comp) );
Inlet.P = sigma (foreach (comp in componentlist) Pfav(comp) );

For comp in ComponentList Do
AveragePressureFeed: Pfav(comp) * (LOGe(Inlet.z(comp) * Inlet.P) - LOGe(Retentate.z(comp) * Retentate.P)) = Inlet.z(comp) * Inlet.P - Retentate.z(comp) * Retentate.P;
AveragePressurePerm: Ppav(comp) * Permeate.F = Jmol(comp) * Permeate.P;
AverageMolFracPerm: Jmol(comp) = Permeate.F * Permeate.z(comp);
Flux:                Jmol(comp) = K(comp) * (Pfav(comp) - Ppav(comp));
ComponentBalance:    Inlet.F * Inlet.z(comp) = Retentate.F * Retentate.z(comp) + Jmol(comp);
EndFor
End
```

## 10.3.2. Model 2

```
// Parameters and variables
NCells      as IntegerParameter (Description:"Number of cross flow cells", 100);
A            as Area             (Description:"Total membrane area", Fixed); // (m2)
L(ComponentList) as Notype       (Description:"Permeability in m3(STP)/(m2 h bar)", Fixed);
Lmol(ComponentList) as Notype    (Description:"Molar permeability (kmol/(m2 h bar))");
PPerm       as Pressure         (Description:"Permeate pressure", Fixed); // (bar)
ACell       as Area             (Description:"Area per cross flow cell (m2)");
FRet([0:NCells]) as Flow_Mol    (Description:"Retentate mole flow from cell"); // (kmol/h)
FPerm([0:NCells]) as Flow_Mol    (Description:"Permeate mole flow from cell"); // (kmol/h)
ZRet(ComponentList,[0:NCells]) as Molefraction (Description:"Retentate mole fraction in cell");
ZPerm(ComponentList,[0:NCells]) as Molefraction (Description:"Permeate mole fraction in cell");
Jmol(ComponentList,[1:NCells]) as Flow_Mol    (Description:"Permeate mole flux in cell");
RhoRet      as hidden Dens_Mol; // Retentate molar density (kmol/m3)
RhoPerm     as hidden Dens_Mol; // Permeate molar density (kmol/m3)

// Ports
Inlet      as Input  MoleFractionPort;
Retentate  as Output MoleFractionPort;
Permeate   as Output MoleFractionPort;

// Convert permeability to molar basis

Lmol = L*101.325 / (273.15*8.314);

// Retentate inlet conditions

FRet(0) = Inlet.F;

For comp in ComponentList Do

    ZRet(comp,0) = Inlet.z(comp);

EndFor

// Balance equations for each cell

ACell = A/NCells;

For k in [1:NCells] Do

    FRet(k-1) + FPerm(k-1) = FRet(k) + FPerm(k);

    For comp in ComponentList Do

        Jmol(comp,k) = ACell * Lmol(comp) * ((Inlet.P*ZRet(comp,k-1)-Retentate.P*ZRet(comp,k))/LOG((Inlet.P*ZRet(comp,k-1))/(Retentate.P*ZRet(comp,k))) - Permeate.P*ZPerm(comp,k));

        FRet(k-1)*ZRet(comp,k-1) + FPerm(k-1)*ZPerm(comp,k-1) = FRet(k)*ZRet(comp,k) + FPerm(k)*ZPerm(comp,k);

        Jmol(comp,k) + FPerm(k-1) * ZPerm(comp,k-1) = FPerm(k) * ZPerm(comp,k);

    EndFor

EndFor
```

```

sigma (foreach (comp in componentlist) ZPerm(comp,k)) = 1;
EndFor

// Retentate total flow and composition
Retentate.F = FRet(NCells);

For comp in ComponentList Do
    Retentate.z(comp) = ZRet(comp,NCells);
EndFor

// Permeate total flow and composition
Permeate.F = FPerm(NCells);

For comp in ComponentList Do
    Permeate.F * Permeate.z(comp) = FPerm(NCells)*ZPerm(comp,Ncells);
EndFor

// Other outlet stream conditions
Retentate.T = Inlet.T;
Retentate.P = Inlet.P;
Permeate.T = Inlet.T;
Permeate.P = PPerm;

Call(Retentate.h) = pEnth_Mol_Vap(Retentate.T, Retentate.P, Retentate.z);
Call(Permeate.h) = pEnth_Mol_Vap(Permeate.T, Permeate.P, Permeate.z);

Call(RhoRet) = pDens_Mol_Vap(Retentate.T, Retentate.P, Retentate.z);
Call(RhoPerm) = pDens_Mol_Vap(Permeate.T, Permeate.P, Permeate.z);
Retentate.v = 1/RhoRet;
Permeate.v = 1/RhoPerm;

End

```

### 10.3.3. Model 3

```
Model GPU2

//ports
Feed as Input MoleFractionPort;
Retentate as Output MoleFractionPort;
Permeate as Output MoleFractionPort;

//dominio
x as LengthDomain (DiscretizationMethod:"BFD1", HighestOrderDerivative: 1, Length:10, SpacingPreference:1);

//distribuicao
Ret as Distribution1D (XDomain is X) of Flow_Mol;
Perm as Distribution1D (XDomain is X) of Flow_Mol;
k(ComponentList) as constant;
yret(ComponentList) as Distribution1D (XDomain is X) of Molefraction;
yperm(ComponentList) as Distribution1D (XDomain is X) of Molefraction;

//eqs
For i in [X.Interior + X.EndNode] Do
    sigma (foreach (comp in componentlist) yret(comp)(i)) = 1;
    sigma (foreach (comp in componentlist) yperm(comp)(i)) = 1;
EndFor

For comp in ComponentList do
    yret(comp)(i).ddx * Ret(i) + Ret(i).ddx * yret(comp)(i) = - k(comp) * (Feed.P * yret(comp)(i) - yperm(comp)(i) * Permeate.P);
    yperm(comp)(i).ddx * Perm(i) + Perm(i).ddx * yperm(comp)(i) = k(comp) * (Feed.P * yret(comp)(i) - yperm(comp)(i) * Permeate.P);
EndFor

//Feed.F = Retentate.F + Permeate.F ;
Ret(0) = Feed.F;
Perm(0) = 0;
Perm(X.EndNode) = Permeate.F ;
Ret(X.EndNode) = Retentate.F;

For comp in ComponentList do
    Feed.F * Feed.z(comp) = Retentate.F * Retentate.z(comp) + Permeate.F * Permeate.z(comp);
    yret(comp)(X.EndNode) = Retentate.z(comp);
    yret(comp)(0) = Feed.z(comp);
    yperm(comp)(X.EndNode) = Permeate.z(comp);
EndFor
End
```

